Dynamic Wave-Soil-Structure Interaction Analysis ---with Applications to Tall Buildings

by

Ming Ming Yao
B.E., Beijing University of Aeronautics and Astronautics, 1999

A Thesis Submitted in Partial Fulfillment of the
Requirements for the Degree of

MASTER OF APPLIED SCIENCE

in the Department of Mechanical Engineering

We accept this thesis as conforming
to the required standard

[redacted]

Dr. Joanne L. Wegner, Supervisor (Dept. of Mechanical Engineering)

[redacted]

Dr. James W. Provan, Inside Member (Dept. of Mechanical Engineering)

[redacted]

Dr. Wendy Myrvold, Outside Member (Dept. of Computer Science)

[redacted]

Dr. Panajotis Agathoklis, External Examiner (Dept. of Electrical & Computer Engr.)

Supervisor: Dr. Joanne L. Wegner

ABSTRACT

This thesis presents a study on Soil-Structure Interaction (SSI) by analyzing the variance of fundamental frequencies and vibration modes of tall buildings through the application of parametric studies. There are two methods available for modeling the SSI: the direct method and substructure method. In this thesis, the substructure method is employed to model the subsystems of unbounded soil and structure separately. The unbounded soil is modeled by using the Scaled Boundary Finite Element Method (SBFEM), an infinitesimal finite-element cell method, [61] which naturally satisfies the radiation condition for the wave propagation problem. The structure is modeled using the standard finite element method. The SBFEM results in less degree of freedoms of the soil than the direct method by only modeling the interface of the interested area. In this work, a Dynamic Soil-Structure Interaction Analysis program (DSSIA) [65] is used and modified to investigate the SSI effect on tall buildings in the frequency and time domains. A parametric study is carried out where the buildings are subjected to external impulse loadings and also earthquake loading. The fundamental frequency and the vibration and peak displacement along the height of the buildings are obtained in the time domain analysis. The coupling between the building's height, hysteretic damping ratio, soil dynamics and SSI effect are also investigated. The results are compared with building codes, field measurements and other numerical methods.

Examiners:

[redacted]

Dr. Joanne L. Wegner, Supervisor (Dept. of Mechanical Engineering)

[redacted]

Dr. James W. Provan, Inside Member (Dept. of Mechanical Engineering)

[redacted]

Dr. Wendy Myrvold, Outside Member (Dept. of Computer Science)

[redacted]

Dr. Panajotis Agathoklis, External Examiner (Dept. of Electrical & Computer Engr.)

Contents

List of Tables

List of Figures

List of Abbreviations

BEM: Boundary Element Method

BLAS: Basic Linear Algebra Subprograms

DOF: Degree Of Freedom

DSSIA: Dynamic Soil-Structure Interaction Analysis

FEM : Finite Element Method

FFT: Fast Fourier Transformation

LAPACK: Linear Algebra PACKage

PD: Peak Displacement

SBFEM: Scaled Boundary Finite-Element Method

SH: Shear Horizontal

SSI: Soil-Structure Interaction

SV: Shear Vertical

UBC: Uniform Building Code

List of Notations

[ ]:Matrix

{ } : Vector

∞ : Infinity

$\{\sigma\}$: stress vector

$\{\varepsilon\}$: strain vector

[D] : elasticity matrix (refer to A.8 [60])

E : Young's modulus

ν : Poisson's ratio

G : shear modulus matrix

subscript b : nodes of the interface

superscript t : total displacement

superscript g : unbounded ground soil with excavation

$\{R_b(\omega)\}$: interaction force on the nodes on the soil-structure interface

$[S^{\infty}(\omega)]$: dynamic-stiffness matrix of the nodes on the soil-structure interface

$[M_{bb}^{g}(t)]$: acceleration unit-impulse matrix

$\{u_b^t(\omega)\}$: displacement of nodes on the soil-structure interface

$\{\ddot{u}_b^g(t)\}$: ground acceleration vector

$\{\ddot{u}_b^t(t)\}$: total acceleration of the nodes along the soil-structure interface

Acknowledgements

Here, I use this chance to express my deep appreciation to Dr. Joanne L. Wegner and Dr. Xiong Zhang, for their warm help and supervision. They guide to explore the beautiful theories and powerful numerical methods in the field of the wave propagation and computational mechanics, respectively. The multi-disciplinary nature of this research involves structural dynamics in civil engineering, ground wave propagation in earthquake engineering and numerical methods in computational mechanics.

I would like to thank Dr. James W. Provan, Dr. Wendy Myrvold and Dr. Pan Agathoklis, for their precious time spent on reading the thesis and their comments and suggestions.

I would like to thank Alma, Dorothy, Marg's help during my study here. And also thank all the members of the Department of Mechanical Engineering at University of Victoria for the friendly and warm support.

Chapter 1

Introduction

1.1 Dynamic Soil-Structure Interaction System

Vibrations of tall buildings are mainly caused by either strong winds or ground motions. In both situations, the mechanism that influences the vibration characteristics of tall buildings is the dynamic soil-structure interaction (SSI), which is mainly governed by soil properties. Due to the soil properties, the boundary condition between the soil and the foundation of the tall building is free. That permits six degrees-of-freedom (DOF): three translational and three rotational DOF for a rigid foundation. The contact between the foundation and the soil is dynamic. In this study, one strong ground motion is used as the input for the wave-soil-structure interaction system.

Seismic waves consist of body waves (such as P-, SH-, and SV- waves) and surface waves (such as Rayleigh and Love waves). The body waves can strike buildings at any arbitrary angle [2] in the half space. A wave is the main energy form in an earthquake, which converts to potential energy due to the elastic deformation, to kinetic energy due to vibration and also to minor thermal energy due to friction. The energy from the incoming wave is transferred to the building through the interaction with the vibrated adjacent soil excited by the wave propagation. The amount of energy transferred to the building is different for waves at different incident angles. In this thesis, the associated response of the building is represented by the peak displacement of the building centerline in the time domain analysis, and is given in Chapter 4.

In an earthquake, the wave reflection and emission from the foundation to the surrounding semi-infinite soil results in energy dissipation. In the SSI system, the outgoing wave will not be reflected back into the system. This dynamic SSI system is a damping system. Compared with a fix-end boundary condition, the fundamental frequency of the tall building with a flexible boundary condition is small and unsteady. The effect of the energy dissipation can be understood by studying the changes of the fundamental frequency and corresponded radiation damping ratio. This part will be addressed in Chapter 3 in the frequency domain analysis.

In Chapter 3, a group of tall buildings, ranging from ten stories to seventy stories, are modeled and their fundamental frequencies and associated radiation damping ratios are calculated by using the DSSIA [65] program in the frequency domain. In a parametric

study, the material properties of the building and soil are shown to influence the response of the building. In particular, the effects of the structural hysteretic damping ratio and soil stiffness are investigated.

The dynamic interaction between the structure and soil is studied by analyzing the time history of the deformation of the entire building and the distribution of interfacial normal stress during a dynamic vibration. The characteristics of the building vibration include, for example, the peak displacement on the superstructure centerline, the maximum stress on the basement wall and further, the stress underneath the foundation mat, which gives the opportunity to calculate the uplift caused by rocking motion of the building. The contact mechanism between the foundations and supporting soil can be modified for improving the earthquake-resistant design of buildings. This information can be used to assess an existing building's vulnerability for the purposes of upgrading the protection measures.

This study of wave-soil-structure interaction will contribute to the understanding of this complex system from the mechanical engineering viewpoint. It will improve the earthquake resistant design of structures in the civil engineering practice.

1.2 Scope of Thesis

First the historical development of soil-structure interaction and the related unbounded soil modeling and structural dynamics are reviewed in this study. In this section, refer-

ences on modeling of tall buildings, unbounded soil, and soil-structure interaction will be reviewed respectively. Because the focus of this research is the soil-structure interaction problem instead of the actual modeling of the structure, a review of methods used to model tall buildings is presented for completeness. The method for modeling the structure is an important field due to the complexity of modeling the vibrating elements, the steel-reinforced concrete, the configuration of the core and the openings in the walls. An introduction to the research in this field is given. For building vibration, the reader is referred to [14]. As stated previously, the modeling of the unbounded soil and the SSI are emphasized in this study.

Due to the focus on the application of the DSSIA program and numerical experiments on investigating the SSI effect in this thesis, the theory of the modeling of unbounded soil can be found in [39]. The governing equations of the unbounded soil are then given in Chapters 3 and 4 respectively.

In the frequency domain, six cases are carried out for buildings with 10, 15, 20, 30, 50 and 70 stories for studying the effect of the SSI. The impulse is applied to the tops of the buildings. In each case, the fundamental frequencies and corresponding radiation damping ratios are obtained and the soil-structure interaction effects are addressed. The relationship between the soil-structure interaction effect and the building heights is studied. This relationship is the dominant factor in determining the free vibration of a tall building. A 50 story building is chosen to investigate further the relationship between the material properties of soil and the dynamic response of a building.

In the time domain, dynamic responses of a tall building with a multi-level basement under realistic seismic excitations including P-, SH-, SV- waves, at various angles of incidence are obtained. The dynamic response of this soil-structure system depends upon frequency content, type and input angle of ground motion, stiffness and height of the building, the number of levels in the multi-level basement and the stiffness of the adjacent soil. The SSI effect on the vibration of the tall building is addressed. Further improvements on modeling the soil-structure interaction are proposed for future research.

Chapter 2

Literature Review

Among the methods for modeling the SSI, there is a huge diversity and mix of methods in the frequency domain (Fourier or Laplace transformation) and the time domain. There are also hybrid methods obtained by combining the finite element method (FEM) [4] and boundary element method (BEM) [15, 63]. These include the interfacial finite element method, the joint element method, or a simple physical model which adopts the spring-dashpot system for representing the interaction between the soil and structure. The building foundation can be modeled as a massless flexible, or rigid plate either lying on the soil surface or embedded in the soil. The interface between the soil and structure is modeled as welded connection by enforcing the same displacement and stress on the interfacial nodes.

2.1 Modeling of Tall Buildings

In the1950 and early 1960 [13, 16, 20], a building was modeled as a cantilever beam with fixed end conditions. In these early studies, a digital computer was first used to solve the analytical equations for vibration of tall buildings and obtain the natural periods and damping ratios. At that time, the discretization method and massive calculations were not popular yet. The computer speed and memory storage limited the accuracy of approximation and the level of complexity of modeling. The method for modeling structural vibration should avoid generating a large amount of DOFs and a large size matrix, such as the mass and stiffness coefficient matrix, in the equation of motion. Other methods were later developed in the past few decades. A simple model of the building using coupled shear plates with openings was applied to investigate the shear wall vibrations and mode shapes for a building damaged in the Alaskan earthquake of 1964 [19]. Under this guideline, other methods such as the finite strip model and the continuum model were developed [3, 8, 21]. All of the above methods result in less DOF. The size of the resulting coefficient matrices is small compared with those using FEM for volume discretization. But these methods lose nonlinear information such as the material nonlinearity and geometrical nonlinearity, and usually are applied only to linear elastic structures. Since a slender structure is significantly nonlinear at large deformation, the small deformation assumption is no longer accurate enough and Hooke's law does not apply. Usually after a strong earthquake, inside structural component failure occurs, such as the failure of welded points and joints between the steel beams, and the dislocation between the steel and attached concrete are often found. These material discontinuities can be modeled as uncer-

tainties in some methods [26]. As a matter of fact, the widely used steel reinforced concrete is a nonlinear material. At the continuum mechanics level instead of the microscale level, the nonlinear properties of the concrete should be taken into account in the modeling.

In recent years, the research on the vibration of the tall buildings is of an increasing interest among the research community. The research on the three dimensional structural dynamics of the vibration of the tall buildings in typhoon active areas such as Hong Kong and Singapore proved that monitoring and controlling the vibration of the tall building is essential for providing a comfortable residential environment [5, 27]. It is important to compare building's natural frequency and the frequency of the wind obtained by local recordings. Researchers in Japan [30, 31, 37] studied the reduction of the vibration amplitude of a tall building subject to a strong wind load or strong earth motion using a hybrid mass damper system. This research focused on vibration control and soil-structure interaction effect in this dynamic system. The buildings are modeled in three dimensions with symmetrical or nonsymmetrical configurations. The nonlinearity of the material properties can be easily included into the beam-column model, which improves the accuracy of this approximation. The fundamental frequencies and corresponding vibration modes are verified by field measurements. The mass damper is used as the vibrating tremor.

Most methods do not include the soil-structure interaction effects when studying the buildings vibration. Some researchers do consider the SSI effects but are limited to a two dimensional analysis [45]. The consideration of the soil-structure interaction effect on the

response of the building in three dimensions is necessary to pursue more accurate results from the viewpoint of engineering practice [46].

In this thesis, the soil-structure interaction of the tall building is investigated and numerically simulated, and the results are compared with building codes, field measurements and results from other numerical methods. The soil-structure interaction effect is investigated and evaluated in the frequency domain and time domains.

2.2 Modeling of Unbounded Soil

Soil constituents exist in solid, liquid and gas states. The solid phase is a mixture of mineral and some organic particles. The gas phase consists of air and water vapor. From experimental results and a mechanical viewpoint, soil shows high nonlinearity and variability in material performance. The nonlinearity of the soil material can be modeled by using a large amount of finite elements. For a large scale case, improving the accuracy requires more finite elements with smaller element size. The coefficient matrix of each element is assembled into the total coefficient matrix of the structure. Furthermore, the matrix and operation procedures demand a huge memory. It may be necessary to write data to the external memory device (hard drive). The data read/write speed is much slower in hard drive than in the RAM. The data transfer between RAM and hard drive slows down the computational processing. The radiation condition, which means the outward propagated wave will not be reflected back into the soil-structure system, is not satisfied by the FEM equations without an artificial transmitting boundary. A linear elastic homogeneous soil is

underground lifelines. Using this assumption, the BEM is widely used in modeling unbounded soil with a transmitting boundary condition for energy radiation [24] (1975). In earlier studies, [38] (1983), [11] (1989), the three dimensional wavefield was composed of a free field and a scattered wavefield. The wavefield was given by solving the Navier's equation in terms of spherical Hankel and Bessel functions, associated with Legendre polynomials [44] (1972), [1] (1980). The radiation condition is satisfied at infinity. But the stress free boundary condition along the surface of the half-space needs to be set locally. In the above methods, the body force is assumed to be equal to zero. Furthermore, the hysteretic damping coefficient can be included by using the complex elastic constants [35] (1982), [17] (1990). The steady-state elastodynamics field equation is used to model the soil which is assumed to be a homogeneous, isotropic and linear elastic solid [7] (1995).

The wave expansion method is used for solving the wave equation for unbounded soil [11]. A scattered wavefield is expressed as a linear combination of wave functions of a free field and a reflected wavefield. By imposing boundary conditions and free-field stresses on the boundary, the coefficient of displacement can be obtained after solving the equations. And furthermore, the displacement and stress fields can be evaluated. There are no stress tractions on the free boundary which is set locally as in the other methods.

Based on the linear elastodynamic theory, a new method was developed by Song and Wolf [40] (1996) and is known as the consistent infinitesimal finite-element cell method. The same equation is obtained for the dynamic-stiffness matrix by limiting the cell width

derived in the scaled boundary finite-element method (SBFEM). In the SBFEM, the dynamic behavior of a unbounded soil is described by using a dynamic stiffness matrix in the frequency domain and the same force-displacement relationship is represented in the time domain by a unit-impulse response matrix.

2.3 Modeling of Soil-Structure Interaction

Extensive literature has appeared in the last two decades on modeling soil-structure interactions. This problem is modeled from many points of view by using advanced numerical techniques such as FEM, BEM, and hybrid methods. As a whole, all of the above methods are an approximate simulation of the real soil-structure interaction with some simplifications. Different methods have different advantages in handling the obstacles which exist for this problem. The methods can be divided into the following groups as follows.

2.3.1 The Analytical Method

Mario E. Rodriguez et. al. [34] (2000) evaluated the importance of SSI effects on the seismic response and the damage of buildings in Mexico City during a 1985 earthquake and compared the results with a rigid case. A simple one degree of freedom model was used for analyzing the overall seismic behavior of multistory building structures built on soft soil. Wolf also used this method to study the vibration of the foundation [55] (1997). The mass-spring-dashpot system is widely used to simulate the interaction of the soil and structure. The analytical method can only be applied to simple structures.

2.3.2 System Identification

Jonathan P. Stewart and Gregory L. Fenves [42] (1998) evaluated the unknown properties of a system by using a pair of known input and known output from the system. A simple spring-mass system was used for the initial interaction. The equations are solved in the Laplace domain by using the parametric system identification method. This method was developed from Luco's method for non-parametric procedure [28] (1980). Fifty-eight sites with instrumentation were investigated for both flexible and fixed boundary condition cases. The responses of the systems to the designed inputs were compared and the SSI effects were addressed. The application of the system identification method in the SSI effect research is efficient.

2.3.3 Nonlinear Soil-Structure Interaction Analysis

The nonlinearities of the interaction between the soil and structure are due to material nonlinearity of the soil and the structure material and geometrical nonlinearity resulting from separation, sliding, and rocking. These nonlinear phenomena usually occur together. The coupling from the uplift, sliding, and rocking are difficult to simulate. In analyzing a nonlinear dynamic response of SSI, the nonlinear impedance method is a modification of the linear impedance method [52] (1976). The time-dependent contact area between the structure base-slab and the soil can be determined. [43] (1976), [33] (1983). The time domain framework is limited to the mat foundation. Wolf [52], Wolf and Skrikerud [59] studied nuclear containment structures including the effects of liftoff and sliding of the foundation basemat. The rocking and normal separation of the foundation and soil is the primary nonlinear interaction effect [33] (1983).

In [57], complete equations were given and the uplift was calculated. A unit impulse matrix was obtained for describing the dynamic response of the soil. In [58], the Green function was calculated and Bessel functions were used. The uplift was examined in the time domain by John P. Wolf and Georges R. Darbre [56]. In this study, the boundary element method was used to model an embedded foundation. The nonlinear material properties of the soil were not considered here. The material properties of the adjacent soil were set equal to those of the nonlinear structure.

Toki and Fu [46] studied a three dimensional stress redistribution of soil based on the Mohr-Coulomb failure law. A generalized method for a full nonlinear earthquake analysis with joint elements was derived for both soil nonlinearity and geometrical nonlinearity, uplift and sliding.

The dynamic process can be simulated at a series of states calculated in each infinitesimal time interval. Hideji Kawakami [25] used an iterative method to simulate the rocking procedure with the modification of the traction and displacement of the foundation and soil. The contact and partial uplift phenomenon were modeled by using a FE model of the surface rigid foundation under the assumption that sliding does not occur.

A time domain equation can be transferred into the frequency domain for easier calculations. The interaction force is derived in the frequency domain. Then it is transferred back into the time domain by using a Fast Fourier Transformation (FFT). Further, the

traction and displacement are modified in the time domain so that the boundary conditions can be set at the interface.

D.B. McCallen [29] designed an interface element to model the interaction between foundation and the soil. The material nonlinearity of the soil and the components of the building were considered. The geometric nonlinearity of the tall building due to large transverse deflections and void formation between the foundation and soil were studied. The soil is unable to support a tensile stress, so the geometrical nonlinearity can occur when uplift occurs.

2.3.4 BEM in Linear SSI

The BEM involved Green's function for the boundary integral equation [9]. By applying the BEM to the unbounded media, it avoided the time consuming finite element implementation of appropriate border elements and finding the necessary finiteness of mass. The Hankel transform of the Navier's equations in each layer was used to determine the impendence of a rigid, surface or embedded circular foundation resting on a halfspace. The continuity of the stress vector and displacement at a given interface was satisfied with the help of transmission and reflection coefficients. Extensive calculations which were required for obtaining Green's function and Hankel transformation were the limitations for these methods.

2.3.5 FE-BE Coupling Method

The FE-BE coupling method for SSI was developed by Karabalis and Beskos [22] (1985), Spyrakos and Beskos, [41] (1986), and Fukui [12] (1987). In later papers [47, 48] (1989, 1988) the structure was modeled as a linear elastic solid using FEM and the half-space was modeled as a homogeneous linear elastic solid using BEM. To satisfy the wave radiation condition, transmitting boundaries were developed [23, 24, 49, 53].

In another study [2], the Fourier transformation was used to transfer the equation of motion into frequency domain for analyzing transient analysis of dynamic soil-structure interaction. In a free field, the displacement is composed of the incident wave, the reflected wave and the scattered wave. In solving the equations describing the scattered wave, the second kind and order zero Hankel function and Green function were applied. The displacement and traction along the interface were obtained.

The coupling between FE and BE is accomplished by invoking the traction and displacement continuity across the interface boundary. The displacement and traction are discontinuous at some portion of the interface.

The limitation in BEM is that only a linearly elastic homogeneous domain can be treated. The structure and a small portion of the supporting soil are discretized by FEM, the rest by BEM. This method ignores the rigid foundation and soft soil contact. Consequently, this type of technique avoids this complex interaction.

2.3.6 Kinematics Soil-Structure Interaction Effects

Due to input soil motion in an oblique direction instead of a vertical direction, a rigid foundation can not accommodate the variability of the motion of the soil [39]. The foundation will average out the variable input motion and subject the structure to the average motion of the foundation. The averaging process depends on the size of the foundation in depth along the direction of the wave travel, and also the wave velocity. Normal complex methods use the radiating or transmitting boundaries in FEM and can take the radiation condition into account. If the foundation is very rigid compared with the adjacent soil, a rocking motion appears. The upper shear strength of the soil may also cause sliding of the foundation block. The rocking and sliding alters the characteristics of the motion compared to the free field. Normal methods assume the foundation is rigidly connected to the adjacent soil and the free field motion is applied to the foundation, or on the shared nodes of interface. The uncertainties in estimating the SSI effect comes from the unknown seismic loading, the variability of soil properties and complex foundation response.

2.3.7 SSI and Torsional Coupling

The torsional response coupled with the SSI for asymmetric building is obtained by using an efficient modal analysis [62]. This method allows a more realistic modeling of the building. However, modelling the SSI effects is more complex using this method.

Chapter 3

Analysis of the SSI Effect in the Frequency Domain

3.1 Methods in Free-Vibration Analysis

There are several methods to obtain the fundamental frequency of a tall building. The natural frequency of the tall building can be estimated by analytical methods [6, 18]; numerical methods; experimental methods such as a wind channel test, a shaking table test; or by field measurement. Among these methods, the analytical methods need ideal assumptions to obtain solutions and therefore there are limitations on using these results. The experimental methods, such as a wind channel test and a shaking table test, are usually expensive and limited by the specific capacity. In the field measurement method, the natural frequencies and the vibration modes are detected from the large amount of field

measurements sampled from the acceleration sensors and displacement sensors installed on the building, and the typhoon or seismic tremor are used as the input vibration sources [36]. Compared with the above methods, numerical methods, such as the FEM, BEM, and hybrid FE/BE method, give promising tools to model the free vibration with soil-structure interaction and are able to solve this eigenvalue problem with a less expensive cost and better accuracy. Using numerical methods, the fundamental frequency, vibration mode, and associated radiation damping ratio can be obtained.

In implementing numerical methods, there are some procedures to model the interaction between the unbounded soil and the structure. So far, researchers developed FEM, BEM, a transmitting boundary method, a hybrid FE/BE method and a scaled boundary finite element method (alias of the infinitesimal finite-element cell element method) [17, 22, 47, 55, 63]. The above methods can be adopted in the direct method and substructure method according to the modeling strategy. In the direct method, the finite element methods can be used to model as large as possible the adjacent soil to improve the accuracy and reduce the reflected wave effect. This method naturally requires a relatively large amount storage and computation time. The substructure method is used to reduce the number of the DOFs of the model by using the scaled boundary finite element on the interface to model the interaction between the soil and the structure. It satisfies the radiation condition for the boundary condition of the unbounded medium, and improves the accuracy of approximation. In this thesis, the substructure method is adopted. The structure is modeled by standard finite elements and the unbounded soil is represented by scaled boundary finite elements.

3.2 Model of the Unbounded Soil

In this thesis, unbounded soil is modeled as one homogeneous, isotropic and linearly elastic material. The stress-strain relationship is simply represented as,

$$\{\sigma\} = [\mathbf{D}]\{\varepsilon\} , \tag{3.1}$$

$$G = \frac{E}{2(1+\nu)} , \tag{3.2}$$

where $\{\sigma\}$ is the stress vector, $\{\varepsilon\}$ is the strain vector, [**D**] is the elasticity matrix (refer to A.8 [60]), E is Young's modulus, ν is Poisson's ratio, and G is shear modulus which can be obtained from a lab test such as a Cyclic Simple Shear Test. Whitman and Richart [51] recommend that Possion's value for sand (dry, moist, partially saturated) to be in the range of 0.35 to 0.4 and equal to 0.5 for clay (saturated). A good value for most partially saturated soil is around 0.4. The soil is one complex phase mixture of solid, water, and air. The engineering behavior of the soil is characterized with a plasticity limit and liquid limit. These important material performances of the soil in the soil-structure interaction will be researched in the next DSSIA version. Herein, the soil is still assumed to be a linear elastic solid.

Unbounded soil is modeled by using the scaled boundary finite element method. This is done by using an infinitesimal finite element cell to model one layer of adjacent soil with the interior boundary coinciding with the interface of the structure, and the exterior boundary representing the rest of the unbounded soil. Representing the force-displacement relationship in the frequency domain and using the theory of similarity, the

dynamic stiffness converges to the value at the interior boundary when the thickness of the layer approaches zero. The force-displacement relationship can be given in frequency domain as, [60]

$$\{R_b(\omega)\} = [S^{\infty}(\omega)]\{u_b^t(\omega)\}, \tag{3.3}$$

where the subscripts b and superscript t represent the nodes of the interface and the total displacement, respectively. The vector $\{R_b(\omega)\}$ is the interaction force on the nodes on the soil-structure interface. The matrix $[S^{\infty}(\omega)]$ is a dynamic-stiffness matrix of the nodes on the soil-structure interface, and $\{u_b^t(\omega)\}$ gives the displacement of nodes on the soil-structure interface. Here the scattered motion of incident waves is zero. More details of this mathematical model can be found in [60].

3.3 Governing Equations of the SSI System

The equation of the motion for the free vibration of the tall building is given by [60],

$$\begin{bmatrix} [S_{ss}(\omega)] & [S_{sb}(\omega)] \\ [S_{bs}(\omega)] & [S_{bb}(\omega)] \end{bmatrix} \begin{Bmatrix} \{u_s^t(\omega)\} \\ \{u_b^t(\omega)\} \end{Bmatrix} = \begin{Bmatrix} 0 \\ -\{R_b(\omega)\} \end{Bmatrix}, \tag{3.4}$$

$$[S^{\infty}(\omega)] = [K](1+2\xi_h i) - \omega^2[M], \tag{3.5}$$

where the subscript s represents the nodes of the structure, [K] is the stiffness matrix and [M] is the mass matrix of the structure, and ξ_h is the hysteretic damping ratio of the structure. The interaction force from soil to the structure's foundation is represented in the

term of $\{R_b(\omega)\}$ in the right term of (3.4). After substituting (3.3) into (3.4) and rearranging the terms, this nonlinear eigenvalue problem [50] can be represented as,

$$\left((1+2\xi_h i) \begin{bmatrix} [K_{ss}] & [K_{sb}] \\ [K_{bs}] & [K_{bb}] + \dfrac{[S^{\infty}(\omega)]}{1+2\xi_h i} \end{bmatrix} - \omega^2 \begin{bmatrix} [M_{ss}] & [M_{sb}] \\ [M_{bs}] & [M_{bb}] \end{bmatrix} \right) \begin{Bmatrix} \{u_s^t\} \\ \{u_b^t\} \end{Bmatrix} = 0, \quad (3.6)$$

The dynamic-stiffness matrix is a frequency-dependent complex matrix, hence (3.6) is more difficult to solve. In [50], this problem is solved by using an inverse iteration method. Using this technique, we can obtain the fundamental frequency and radiation damping ratio when the hysteretic damping ratio of the structure is set equal to zero.

3.4 DSSIA

The DSSIA program [65] is a solver for the 3-dimensional dynamic soil-structure interaction problem. The ALGOR software is applied to complete the modeling and discretization. The coordinate of each node and element information are read by the application ALGDSS.EXE and formatted as input data for DSSIA.EXE. An example of some input data is given in Appendix C. Further detailed information about the input data format can be found in the DSSIA Manual [64]. According to different demands of the design, the free vibration analysis in the frequency domain or the dynamic response in the time domain can be assigned by setting a control variable in the control line of the input data. By using the FFT, the dynamic relationship can be represented as an eigenvalue problem in the frequency domain. After solving this eigenvalue problem, the fundamental frequency, vibration mode and damping ratio are obtained.

One of my efforts was to analyze the computer code and understood the program in order to modify it. The DSSIA is composed of the main program DSSIA.F and subroutines. The solving of the eigenvalue program is accomplished by LAPACK, which is a linear algebra library available online (http://www.netlib.org/lapack/index.html). LAPACK is the acronym for Linear Algebra PACKage. It is written in Fortran 77. The LAPACK routines do computations by calling routines in the Basic Linear Algebra Subprograms (BLAS). The LAPACK routines are based in the Level 3 BLAS which provide matrix multiplication. The LAPACK provides either single or double precision. In DSSIA, the double precision is used.

3.5 Numerical Studies

In order to investigate the effect of the soil-structure interaction, six cases are considered for buildings with 10, 15, 20, 30, 50, and 70 stories. A harmonic impulse is chosen as the input load applied to the tops of the buildings (Figure 3. 1). Fundamental frequencies and radiation damping ratios are compared and the soil-structure interaction effects are addressed. First, the relationship between the soil-structure effect and a building's height is studied. The effects of the coupling of the mass moment of inertial of the building with the soil-structure interaction on the free vibration of the tall building is investigated. Second, for a specific case, the 50 story building is chosen to further study the relationship between the material properties of soil and the structure. The soil's shear modulus, (3.2), is changed with the properties of the building held constant. From this case study, the influence of the soil's shear modulus on the response of the building is addressed. This also

can be called the performance variance of soil on the influence of the soil-structure interaction effect. Third, the relationship between the structural hysteretic damping ratio and the response of the building is studied. These studies may contribute to the understanding of the soil-structure interaction effect and upgrading a building's resistance to vibration. This information will be useful for the design of new buildings.

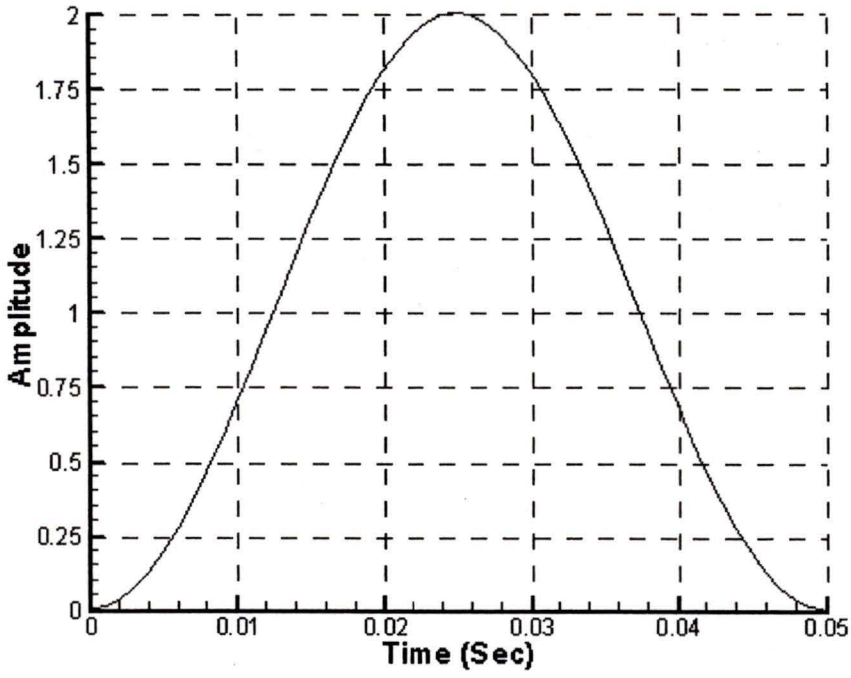

Figure 3.1 The impulse is added on the top of the building as the input load. The amplitude is non-dimensional.

3.5.1 SSI and the Building Height

The fundamental frequencies and associated damping ratios for two groups of models, with or without 5-level basements, are given in figure 3.2. And the fundamental frequency calculated from the Uniform Building Codes (UBC) codes are also given as a reference in Figure 3.2.

First, from the fundamental frequency distribution, for the flexible boundary condition case, the fundamental frequency decreases as the building's height increases. There are differences between the results calculated and the UBC formula, especially at the lower levels. As the number of floors in the building increases, this difference decreases. The influence from the soil-structure interaction decreases for higher buildings. Second, the

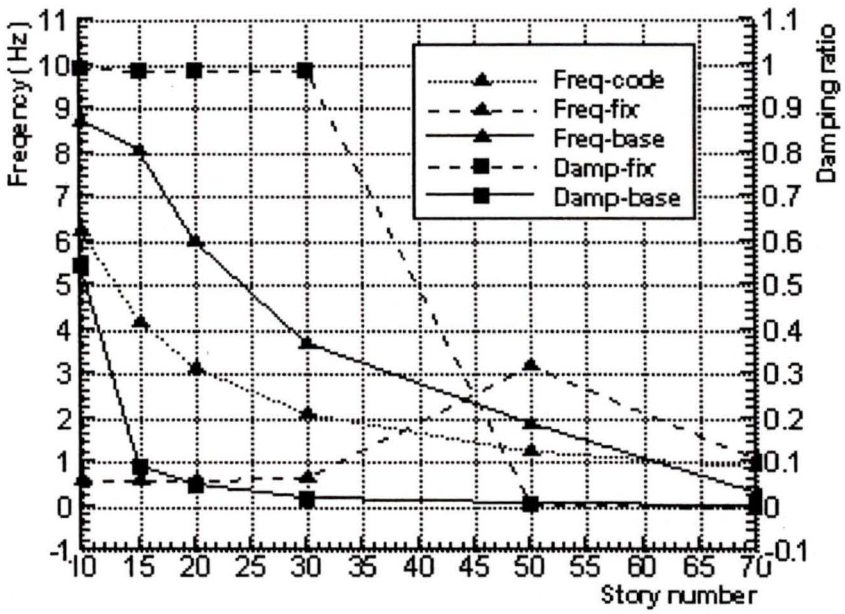

Figure 3.2 Fundamental frequency and radiation damping ratio vs. story number. The frequencies are calculated for buildings with flexible or fixed end conditions and are compared with the results from Uniform Building Code formula.

radiation damping ratio for the building with basement decreases from 0.54% to around zero at the 70-story level. The radiation damping ratio is inversely proportional to the fundamental frequency of the building's response. The radiation damping ratio increases as the fundamental frequency decreases. The imaginary part of the vibration, which represents the energy dissipation, also depends on the fundamental frequency. The lower building experiences a shorter time to dissipate the kinetic energy. The taller building has a longer response time. The relationship between the fundamental frequency and the build-

ing height is also shown in Figure 3.3, which is the visualization of the measurement in Table 3.1. Generally, the lower building has a higher fundamental frequency and radiation damping ratio. The SSI effect reduces the fundamental frequency of the vibration of the highrise building. For identical soil properties, the different height buildings have different degrees of response.

Table 3.1. Measured natural frequencies of different height buildings

	Number of stories	Measured period		Measured frequency	
		Short side	Long side	Short side	Long side
North Hollywood Federal	6	0.79	0.59	1.27	1.69
Airport Control Tower	12	0.88	0.91	1.14	1.1
Tishman-Flower	20	1.75	1.6	0.57	0.625
Travelers Insurance	22	2.1	1.5	0.48	0.67
Barrington Plaza	26	2.12	1.74	0.47	0.57

(S.R. K. Nielsen, 1989, 45, TABLE 5, [32])

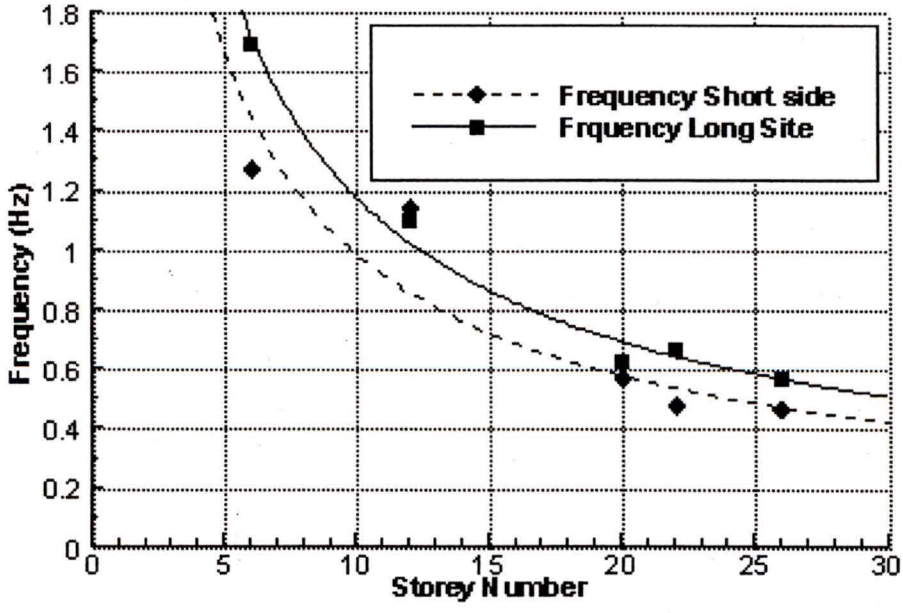

Figure 3.3 Field measurements of tall buildings

3.5.2 SSI and Soil Dynamics

In order to study the influence of the soil material performance to the response of a tall building, a 50-story above ground building with a 5-level basement is used as a detail

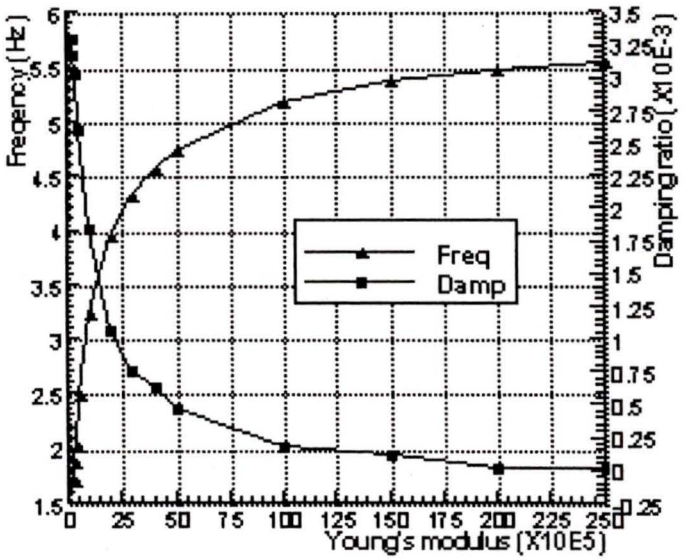

Figure 3.4 Fundamental frequency and radiation damping ratio of 50-story building with 5-level basement.

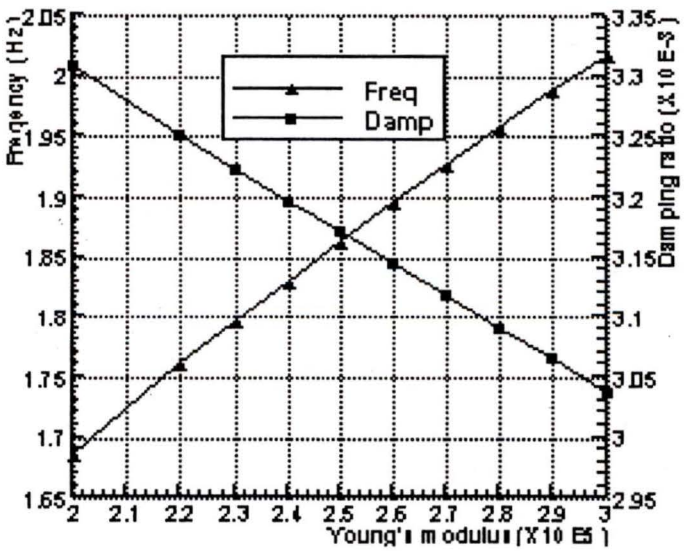

Figure 3.5. Fundamental frequency and radiation damping ratio of 50-story building with 5-level basement in soft soil.

case study. As shown in Figure 3.4, the vibration of the building has a lower fundamental frequency in more soft soil. When the soil's elasticity is small in comparison to the building, the relationship between the soil's Young's modulus and the fundamental frequency of the building becomes proportional (Figure 3.5). The building's response is very sensitive to the changes of soil's elasticity, especially in a soft site. For real soil around the building foundation, the soil's stiffness would increase when experiencing the load-unload loop caused by the building's vibration. The fundamental frequency would accordingly change from a lower frequency to a higher one. Sometimes, the soil can become loose. Even liquefaction would occur under the condition of resonance. The building would partially lose the soil's support and the fundamental frequency also would be reduced. In fact, the building's response is complex and sometimes unpredictable since the influencing factors are variable and dynamic. Conversely, as the soil's elasticity increases, the damping ratio decreases. This relationship is represented in the solution of the eigenvalue problem. For example, the first vibration mode can be written as [50] ,

$$\omega_1 = a_1 + b_1 i, \tag{3.7}$$

$$\xi_1 = b_1 \Big/ \sqrt{a_1^2 + b_1^2}, \tag{3.8}$$

where a_1 denotes the fundamental frequency, subscript 1 represents the first mode and ξ_1 is radiation damping ratio of the first vibration mode.

From Figure 3.4, the fundamental frequency reaches an upper limit as the stiffness of the adjacent soil approaches the value of the stiffness of the structure. At the same time, the

soil's influence on the response of the structure becomes less. The fundamental frequency is close to the results obtained for the fix-end boundary condition.

As mentioned above, the elasticity of the adjacent soil can influence a building's response. In a real event, the other material performances and engineering behaviors would change as a function of both the loading and the time. The dynamic response of the building is specific to the soil properties at the building site. The influence of the soil's dynamics on the vibration of the building is extremely important for understanding the soil-structure interaction.

3.5.3 SSI and the Hysteretic Damping Ratio of the Building

Because of the non-homogeneous nature of the building, with large magnitude vibrations, the building would lose its elasticity to some degree due to the yielding of the concrete, broken weld joints and other structural failures. The hysteretic damping ratio would increase under this assumption. As shown in Figure 3.6, when the hysteretic damping ratio changes from 0 to 0.5, the fundamental frequency changes from 1.864Hz to 2.045Hz. The damping ratio also increases. From the solutions of the eigenvalue problem, the damping ratio includes the hysteretic damping ratio of the structure and the radiation damping ratio, when the hysteretic damping ratio of the structure is not zero. Then the damping ratio becomes an equivalent ratio instead of the radiation damping ratio. So when the hysteretic damping ratio increases, the damping ratio also increases. In a high-rise building, except for the specification of the site soil and structure properties, the hysteretic damping ratio

influences the energy dissipation mechanism between the SSI system and the unbounded soil.

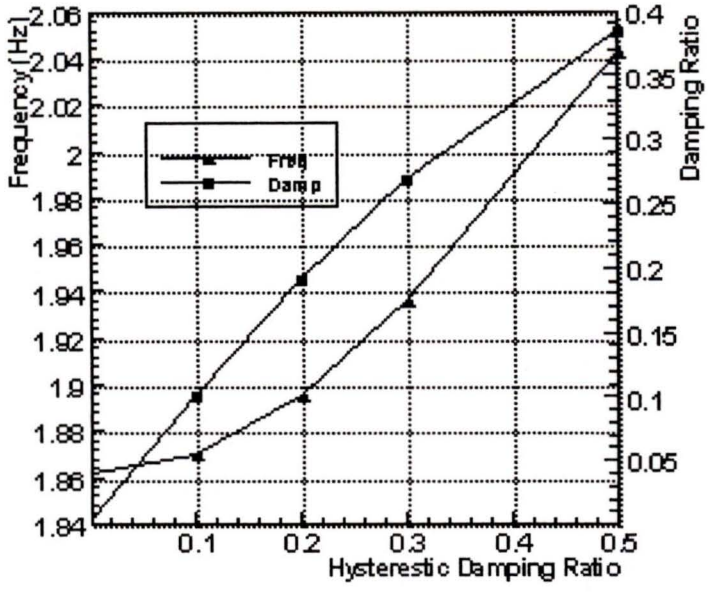

Figure 3.6. Equivalent damping ratio and fundamental frequency for 50-story building with 5-level basement.

3.6 Conclusions from the Frequency Domain Analysis

The relationship between the soil-structure interaction and the possible influential factors such as the building's height, soil dynamics, and structure's hysteretic damping ratio is investigated by using the DSSIA program. The response of the building depends on the material properties of the soil and the structure. In sites with soft soil, the building has a low fundamental frequency, which is sensitive to the change of the soil's rigidity. Because the mechanical behaviors of the soil are changed by the dynamic load-unload loop from the vibration of the building or the earthquake waves, accordingly the damping ratio is also influenced by the changes of the soil's rigidity reversely.

On the other hand, the structure's hysteretic damping ratio influences the fundamental frequency and the equivalent radiation damping ratio. As a result, the fundamental frequency of the building represents the soil-structure system's response and the associated damping ratio represents the energy dissipation of the system to the unbounded soil.

Chapter 4

Analysis of the SSI Effect in the Time Domain

In this part, we apply the DSSIA program to obtain the dynamic response of a tall building with multi-levels basement under realistic seismic excitations including P-, SH-, SV-waves, at various angles of incidence [66]. Tehranizadeh [45] obtained results for this problem using a direct method. The dynamic response of this soil-structure system depends upon frequency content, type and input angle of ground motion, stiffness and height of the building and the number of basement floors.

The response of a tall building's vibration after impact by a large seismic motion is of extreme interest to the research community. Recent literature on this subject obtains results using the direct method. The results show that the adjacent soil is an important factor on the amplitude of structure's motion and damping ratio. In order to achieve the

proper accuracy and to reduce the effect of the reflected wave by the transmitting boundary, it is necessary to consider a large amount of soil around the structure.

In the Dynamic Soil-Structure Interaction Analysis program, the substructure method is employed, and the scaled boundary finite element method is used to model the soil-structure interface. The DSSIA program has the ability to model the input dilatational and shear waves using artificial harmonic waves or seismic recordings. But the Rayleigh wave is only applicable for harmonic wave input according to the current version of DSSIA. Therefore, in this thesis, the P, SH, and SV waves are considered as the input

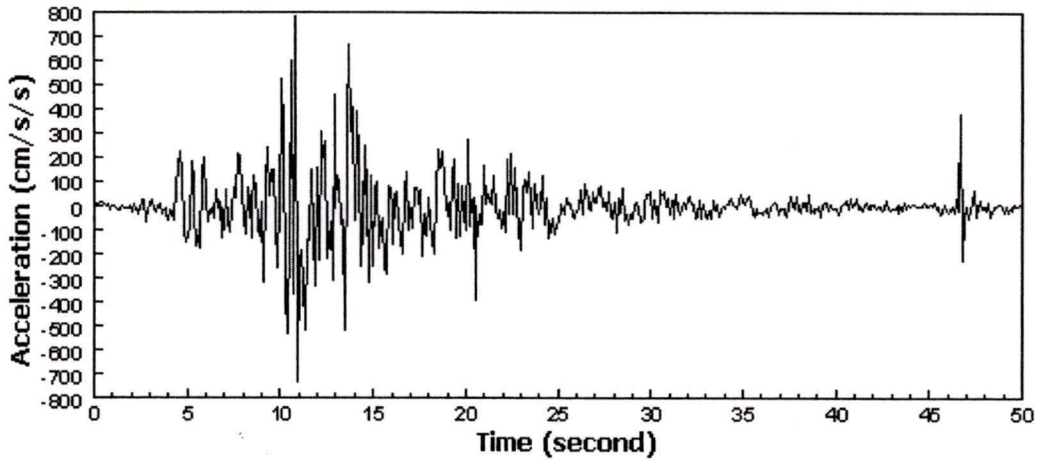

Figure 4.1 Tabas earthquake records (Iran, 1978.09.16)

waves, respectively, based on the Tabas earthquake recording, which was also used in the study by Tehranizadeh [45]. The Rayleigh wave is investigated as a case study for the harmonic wave.

The substructure method reduces the amount of the degrees of freedom (DOF) for the three-dimensional finite element analysis model because less soil is modeled. Thus it is convenient for running a three-dimensional FE program even on a relative low performance PC system because of the smaller requirement for computer memory and run time.

4.1 Governing Equations in the Time Domain

The equation of motion of the SSI system can be given as [Wolf, 1988]:

$$\begin{bmatrix} [M_{ss}] & [M_{sb}] \\ [M_{bs}] & [M_{bb}] \end{bmatrix} \begin{Bmatrix} \{\ddot{u}_s^t\} \\ \{\ddot{u}_b^t\} \end{Bmatrix} + \begin{bmatrix} [C_{ss}] & [C_{sb}] \\ [C_{bs}] & [C_{bb}] \end{bmatrix} \begin{Bmatrix} \{\dot{u}_s^t\} \\ \{\dot{u}_b^t\} \end{Bmatrix}$$
$$+ \begin{bmatrix} [K_{ss}] & [K_{sb}] \\ [K_{bs}] & [K_{bb}] \end{bmatrix} \begin{Bmatrix} \{u_s^t\} \\ \{u_b^t\} \end{Bmatrix} = \begin{Bmatrix} 0 \\ -\{R_b(t)\} \end{Bmatrix} \tag{4.1}$$

where $[\boldsymbol{M}]$ is the mass matrix, $[\boldsymbol{C}]$ is the damping matrix, $[\boldsymbol{K}]$ is the stiffness matrix of the structure, $\{\boldsymbol{R}_b(t)\}$ is the interaction force vector, $\{\boldsymbol{u}\}$ is the displacement vector, $\{\dot{u}\}$ is the velocity vector; and $\{\ddot{u}\}$ is the acceleration vector. The subscripts b and s represent the nodes on the soil-structure interface and the nodes of the building, respectively, and the superscript t represents the total motion of the structure.

The significant portion of the solving procedure is the calculation of the interaction force. In the substructure method, the force is expressed as a convolution integral [60]

$$\{R_b(t)\} = \int_0^t \left[M_{bb}^g(t-t)\right]\left(\{\ddot{u}_b^t(t)\} - \{\ddot{u}_b^g(t)\}\right)dt \tag{4.2}$$

where superscript g means the unbounded ground soil with excavation, $[M_{bb}^g(t)]$ is the acceleration unit-impulse matrix, and $\{\ddot{u}_b^g(t)\}$ is the ground acceleration vector and

$\{\ddot{u}_b^t(t)\}$ is the total acceleration of the nodes along the soil-structure interface. In [65] more details on calculation procedures are provided. The model and assumptions of this SSI governing equation can be found in [60].

Combining (4.1) and (4.2) and discretizing the system in the time and space domains, the acceleration, velocity and displacement are solved and integrated at each time step. The entire solution procedure is the core of the DSSIA program, which is employed as the solver of the finite-element method for analyzing the tall building's response, subject to the input seismic recordings.

The damping factor, the 2nd term on the left-hand side of (4.1), is not considered in this thesis in the time domain analysis. For the analysis of the fundamental natural frequency and the corresponding vibration mode shape, the damping ratio will be considered in the frequency domain.

4.2 Modeling in Time Domain

In considering geological problems, usually large amounts of soil need to be modeled in the FEA. In the substructure method, we use the scaled boundary element method to discretize the interface between the structure, including the wall of the basement and the foundation of the building, and the adjacent soil. So the number of DOFs of the system is reduced by an order of magnitude compared to the direct method. The most DOFs are used to model the building structure instead of the soil. Therefore finite element and cur-

vilinear elements can be used to model the tall building with the goal to improve the accuracy of the approximations.

In order to obtain the building's deformation in an earthquake simulation, the superstructure model is simplified with uniform properties in each cross-section and along the height of the building. The resulting model of the SSI system is composed of one three-dimensional column and the discrete boundary around the basement levels. By using the numerical method to investigate the building's response, the conceptual overall deformations about the tall building by severe ground motion are obtained.

In an actual experiment by using a test table to simulate the ground motion, the input motion is usually along two orthogonal horizontal directions and one vertical direction in the acceleration-time history data. In this numerical study, the scheme is to assign the input body wave with an angle measured from the horizontal, in order to simulate real wave motion in the unbounded medium. In the surface wave case, such as a Rayleigh or Love wave, harmonic motion is used. Because the surface waves can result in the most devastating building destruction, it is important to study the effects of these waves on the structures.

The tall building model is designed with 30 stories above the ground and 5 basement levels. Each level is $18 \times 18 \times 3.5\text{m}^3$ and is discretized into elements $3 \times 3 \times 3.5\text{m}^3$. Consequently, each level has 36 elements. The total structure elements for the 35-story building will be $6 \times 6 \times 35$. The building element is an 8-node brick element. Each node has 3 de-

gree of freedoms for translational movement in Cartesian coordinate space. The interface element is a plate element with node coincidence with the one of the structure's elements. The SSI interface is divided into three parts; the surface of the first two level basements the remaining three levels with the adjacent soil, and the interface between the foundation and the underneath soil. There are 6 × 4 × 2 and 6 × 4 × 3 plate elements with the surrounding soil respectively, and 6 × 6 × 1 plate elements contacting with the underneath soil. There are total 156 plate elements and 1260 brick elements, and the total nodal nodes are 1764. The stiffness matrix has 1764 × 3 DOFs.

In order to obtain the response of different tall buildings subjected to the same seismic recordings, 5-, 10-, and 20-story buildings were modeled and calculated; each with 5-level basements. The 5-, 10-, 20-, and 30-story buildings are noted as models A, B, C and D, respectively, in this thesis.

Soil properties are assigned to the nodes on the interface with the building. The soil properties can vary according to the different layers. In this study, the building's overall displacement is of most interest. The dynamic response of the building is dependent on the soil properties and damping ratios of soil and building.

4.3 Numerical Studies

The first study investigates the response of the 30-story building, including a 5 level basement, subjected to P, SH, SV waves from 90, 60 and, 30 degrees measured from the

horizontal direction. Each story's displacement amplitudes are obtained and compared between different input angles for one input wave type or between different wave types. The building is assumed to stand on the soft soil instead of fixed or semi-fixed on a rock bed. In this study, we use the consistent mass matrix without mass lumped damping as mentioned above.

The origin of the Cartesian coordinate system is assigned to be at the center of the first level, where the building intercepts with the ground surface. The building is symmetric about the coordinate planes, X-Z and Y-Z. The X-Y plane is parallel to the ground surface and the Z-axis is pointing downward into the half space. We select the X-Z plane as the input plane without loss of the generalization. The input angle is measured from the X-axis positive direction to the wave transfer direction. For inputting the seismic recordings, the control point is coincident with the original point of the coordinate system.

Then the other three models are studied, and their displacement amplitudes along the height distribution with the 30-story building, subjected to same input motion, are compared. The effects of the building's configurations on the influence of its vibration and deformation in the event of simulation are obtained. This can be explained by at the site impacted by severe ground motion, buildings of different heights experience different damage. Usually, the most damage happens to the middle size residential buildings because of their small inertial moments, which cause the buildings' fundamental frequencies to lie in the earthquake low frequency intervals resulting in weak resistances to vibration.

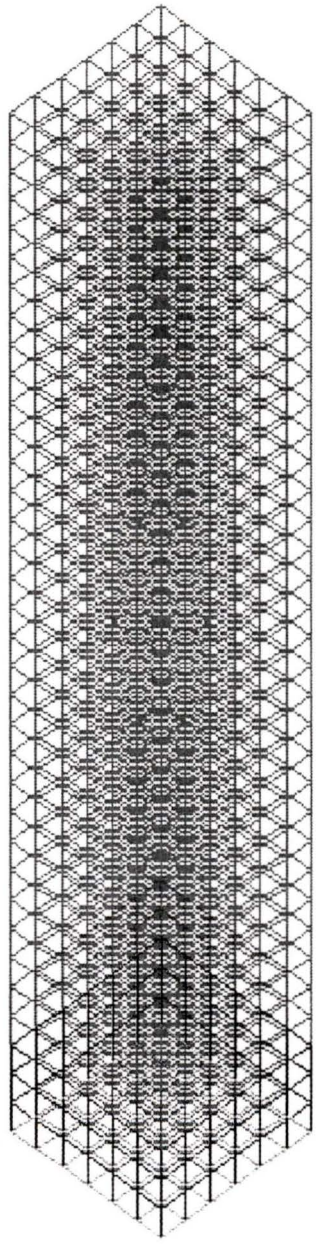

Figure 4.2 Finite element model of 30 story building with 5 level basement. The green, red, and yellow layer represent the upper soil layer, lower soil layer and underneath soil layer, respectively. The soil layer is modeled by using the scaled boundary finite elements which share the same plate element of the structure. The blue elements are the structural brick elements.

By using the dynamic analysis in the frequency domain, the natural frequency and corresponding vibration mode shape can be obtained in a future study. In this study, the dynamic linear elastic analysis is carried out for tall buildings. The torsional movement will not be given in this study and the bending of the building will be expressed as equivalent translational displacement

4.4 Results and Interpretations

In this part the simulation results are reasonably interpreted in detail. The peak displacements (PD) are used to analyze the dynamic behavior of the tall building in the excitation of seismic motion. This result is different from the displacement contour along the height at a sample time point. The displacements of the nodes are relative to the static position before seismic motion is introduced to this simulation system.

4.4.1 Case Study for 30-Story Building

4.4.1.1 P Wave

With a vertical P wave (measured 90 degrees from the horizontal), the largest displacement occurs along the vertical axis. In Figure 4.3, the basement has the largest amplitude of displacement. The displacement decreases from the ground level to the 28^{th} level, then the value becomes steady to the roof. The dilatational wave transfers the energy through the stress generated in the building, after the foundation is stressed by the vertical input wave. Because the model is axially symmetric, the horizontal displacements in the X and Y direction are the same. The horizontal displacement amplitude is about 50 times less

than the vertical axial deformation. When the building shakes, the horizontal PD changes from 44 to 18 in nondimensional units, then back to approximately 47 at the 2nd level from the ground. This matches the horizontal axial largest deformation that usually happens around the ground levels in an earthquake. From Figures 4.3-4.5, the Y direction amplitude of the displacement of the node in the centerline of the building keeps this trend. The PD along the X direction increases to the same magnitude as the vertical PD when input angle is 60 degrees; and to the triple of the vertical PD when the input angle is 30 degrees, which is closer to the horizontal plane. Since the seismic input plane is the X-Z plane, the X direction is influenced more than the Y direction. The energy dissipated by the inter-story drift also increases. When the P wave impacts the building with the smaller input angle, this results in larger displacement and consequently, more damage. Therefore, building damage will vary according to the value of the input angle of the dilatational wave.

4.4.1.2 Shear Wave---SH, SV

The SH wave is a shear wave with the particle motion direction parallel to the ground surface, and vertical to the X-Z input plane. For an input angle of 60 degrees, the main component of the deformation occurs in the Y direction. The building absorbs the kinetic energy with large deformations on the base. As shown in Figure 4.6, the PD is at a maximum at the 3rd level of the basement, decreases proportional to the height from the ground level to the 13th level, and then after increasing, quickly decreases to zero.

The X, Z displacement is a much smaller component, which can be neglected. In the case of SV input waves, the X, Z component are the main components of deformation; the Y direction becomes less than 100 times than in other directions. The SV is a shear wave with particle movement in a plane vertical to the ground surface and coincident with the X-Z input plane. As a result, most of the energy will be dissipated in the input plane along the X, Z directions. As shown in Figure 4.7, the maximum PD of X occurs at the ground level and then decreases with a large slope from 3450, in nondimensional units, to 350 from the 5^{th} to 15^{th} level

4.4.1.3 SSI Effect

From this analysis, the SSI effect is demonstrated by the distribution of PD obtained in the analysis at the underground level. Because of the interaction between the structure and the adjacent soil, the deformation of the building is influenced by the dynamic effect of the soil. Consequently, the peak values of deformation usually occur at the ground level, which is at the boundary between the soil and the free surface.

Different wave types result in deformation of the building in the main energy transfer direction. This can be explained as the impact phenomenon. Axially symmetric buildings such as cylinders, prisms and square section columns have shown to be the most resistant to the severe ground motion. Also, the building above the ground needs to be more flexible as the height of the building increases.

4.4.2 Building Factor

In order to compare the contribution to the damage of buildings at different heights, and for different types of input ground motion, the models A, B, C and D are investigated, respectively, for different types of input ground motion.

For the P wave, for the case of an input angle of 60 degrees, the basement level has a more complex deformation than for the vertically input motion as mentioned before. The shorter height building has a larger PD in the vertical direction, as shown in Figures 4.8-4.9. The most influenced building height is approximately in the range from 10-stories to 15-stories. The foundation uplifts contribute more to the translational displacement in the movement of the center line nodes. By comparing the X direction deformations, it shows that a shorter height building has a greater horizontal drift than taller buildings.

As shown in Figures 4.10-4.11, for both shear waves, the models B, C and D have similar slopes in the peak displacement along the horizontal directions, X or Y, when at the 60 degrees input angle. The model A has the same slope when the input wave is a SH wave. It has a large drift that can be verified from the displacement-time history of the roof center. This study is carried out for checking the building's response at different heights at one earthquake event.

4.4.3 Time History of Roof Movement

The vertically input P wave case is illustrated in detail here. As shown in Figure 4.12, models A and B begin to move from the static position at approximately 13 seconds and 22 seconds, respectively. The taller buildings C and D begin to be move around 25 and

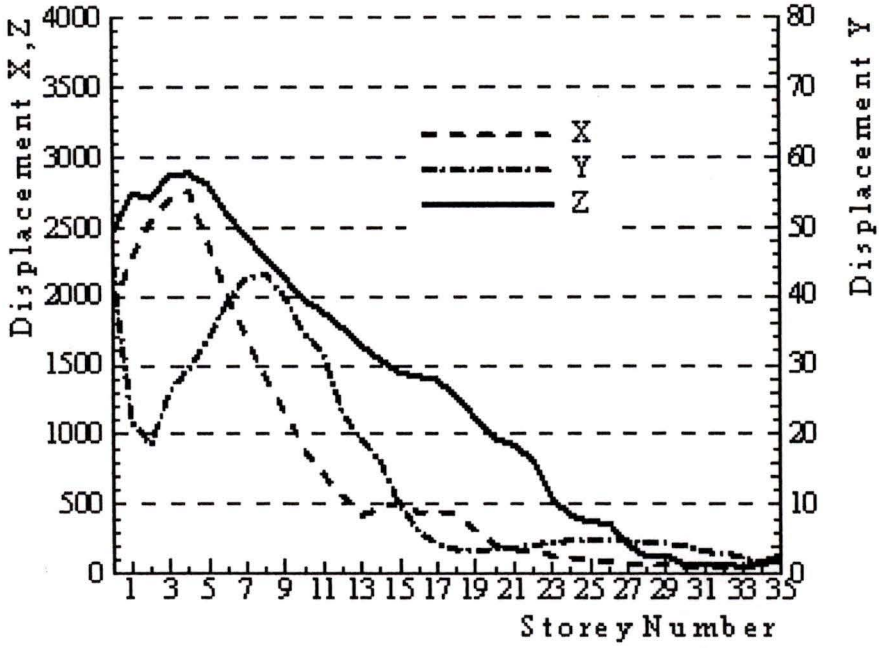

Figure 4.4. Peak displacement of the centerline of model D by P wave at 60 degree input angle

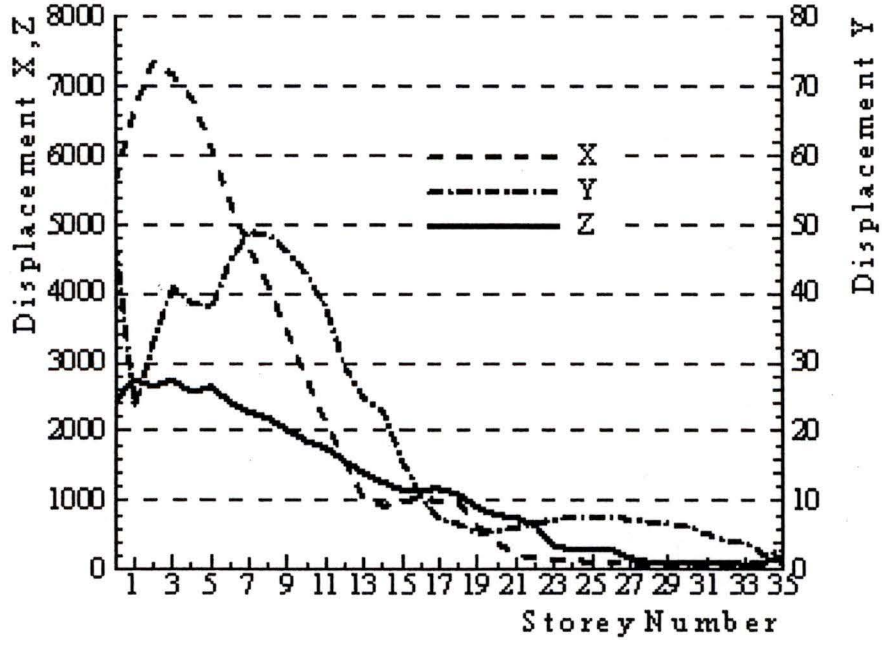

Figure 4.5. Peak displacement of the centerline of model D by P wave at 30 degree input angle.

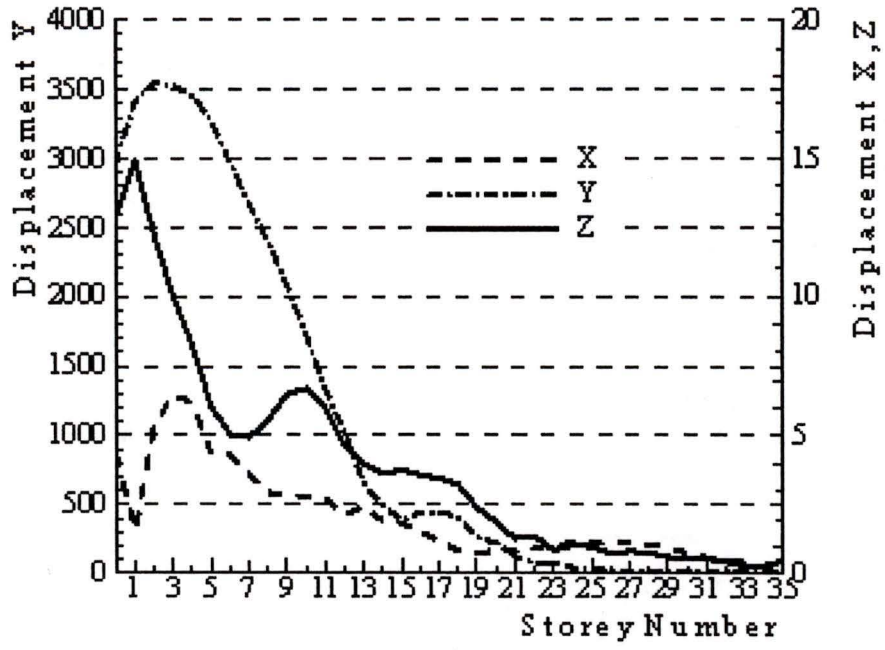

Figure 4.6. Peak displacement of the centerline of model D by SH wave at 60 degree input angle

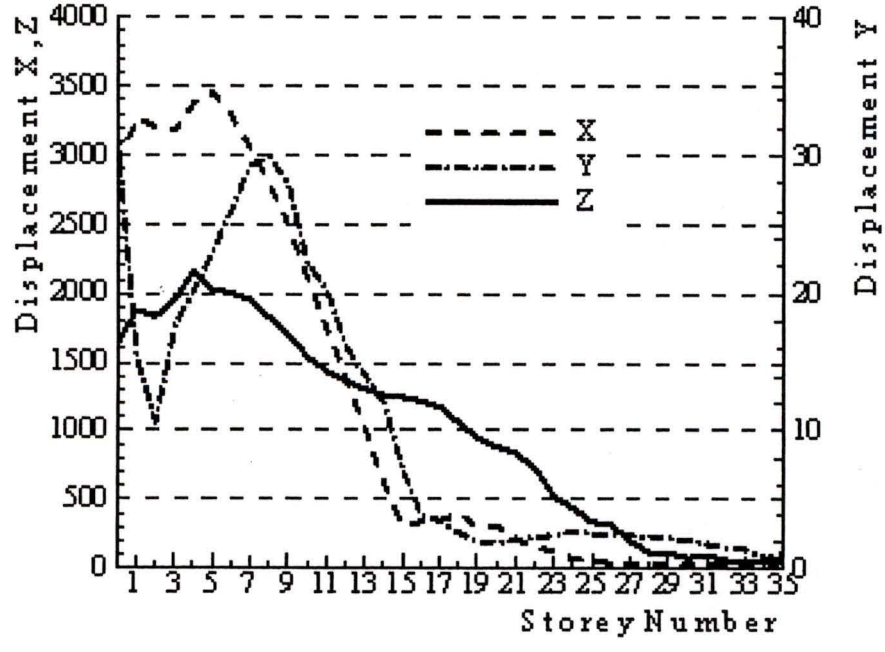

Figure 4.7. Peak displacement of the centerline of model D by SV wave at 60 degree input angle

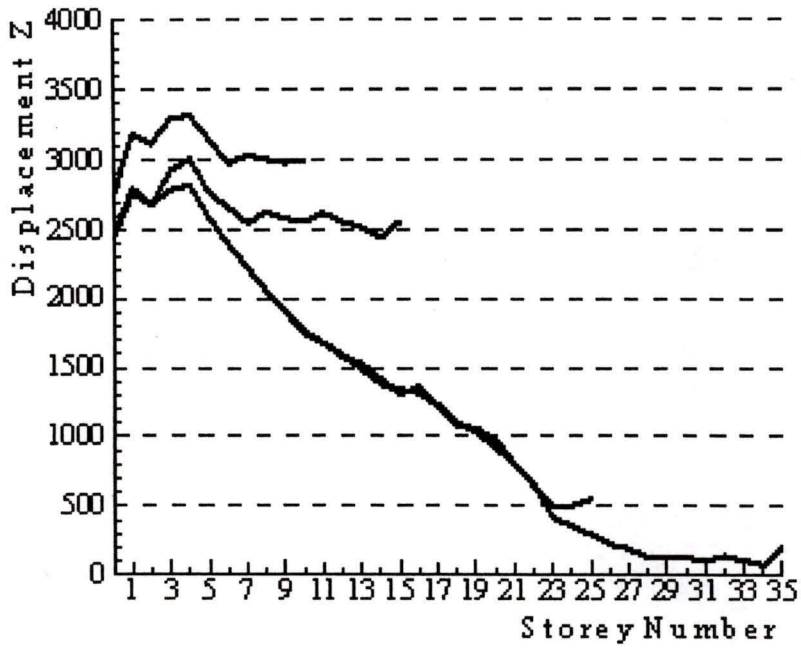

Figure 4.8. Displacement of node in the centerline of models by vertically input P wave.

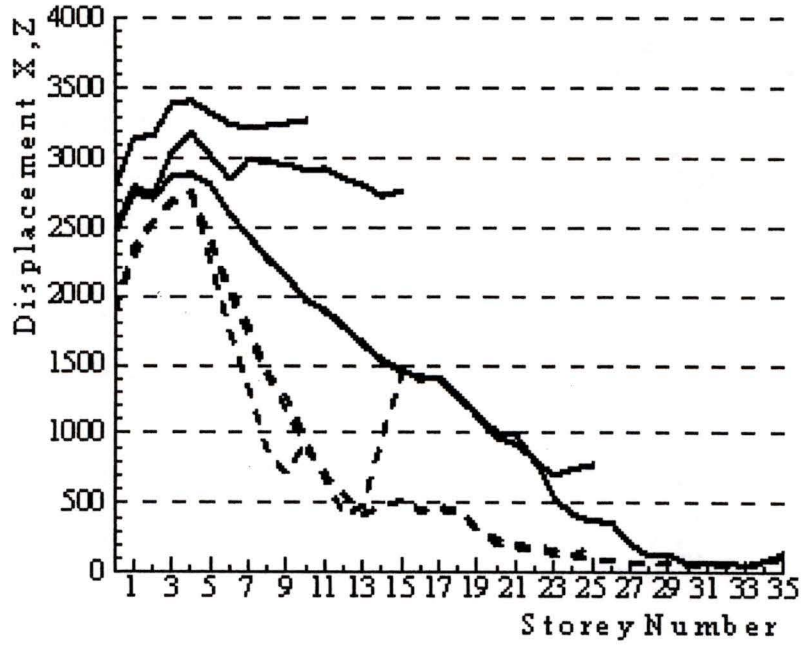

Figure 4.9. Displacement of node in the centerline of models by P wave at 60 degree input angle

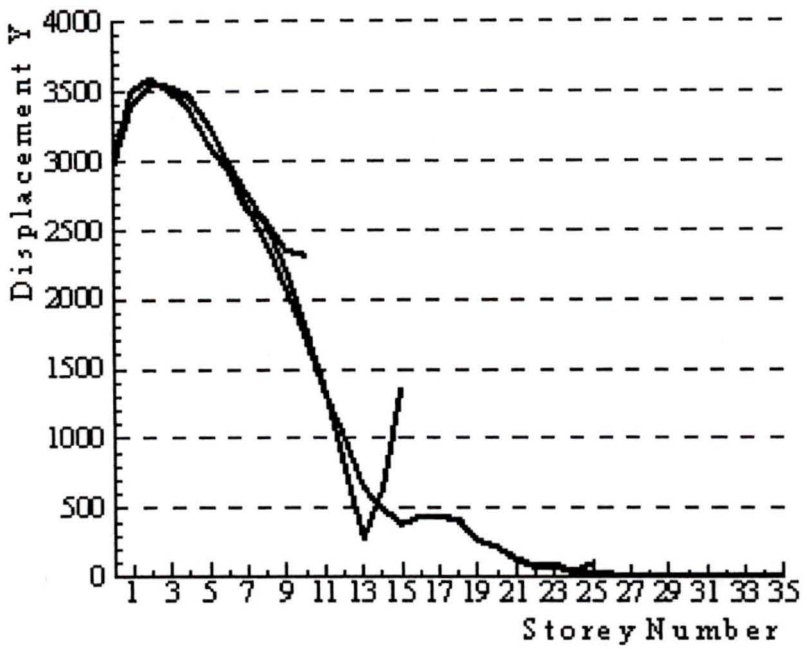

Figure 4.10. Displacement of node in the centerline of models by SH wave at 60 degree input angle

Figure 4.11 Displacement of node in the centerline of models by SV wave at 60 degree input angle

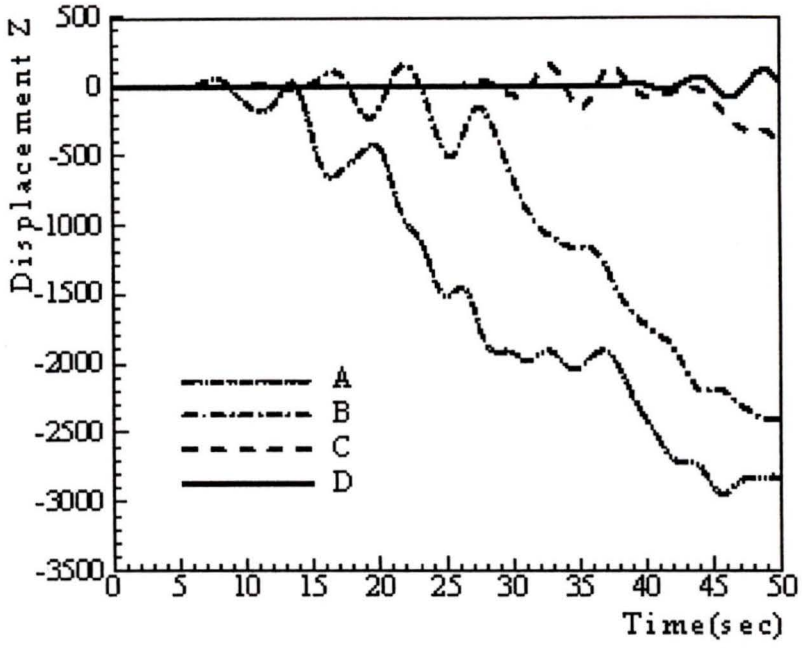

Figure 4.12. Time history of the displacement for the roof center of the buildings.

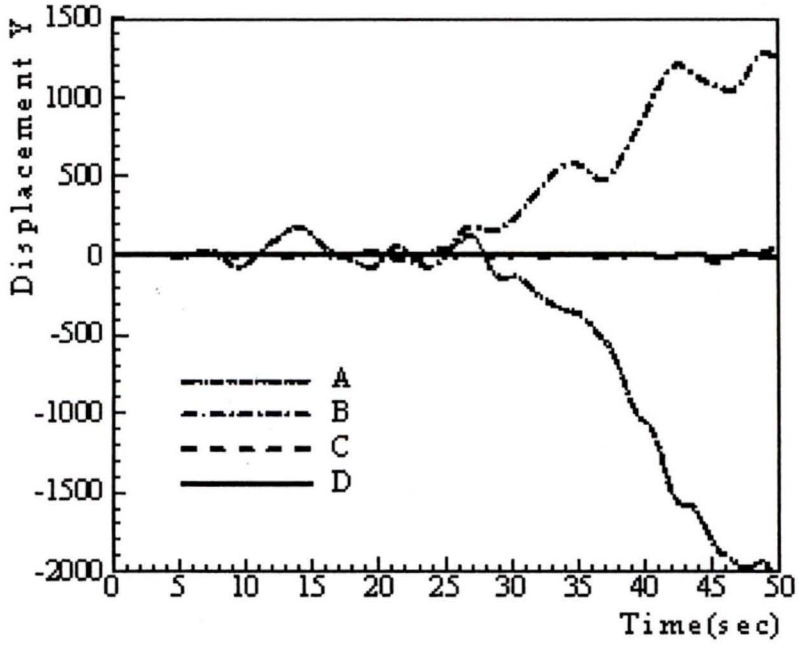

Figure 4.13. Time history of the displacement for the roof center of the buildings.

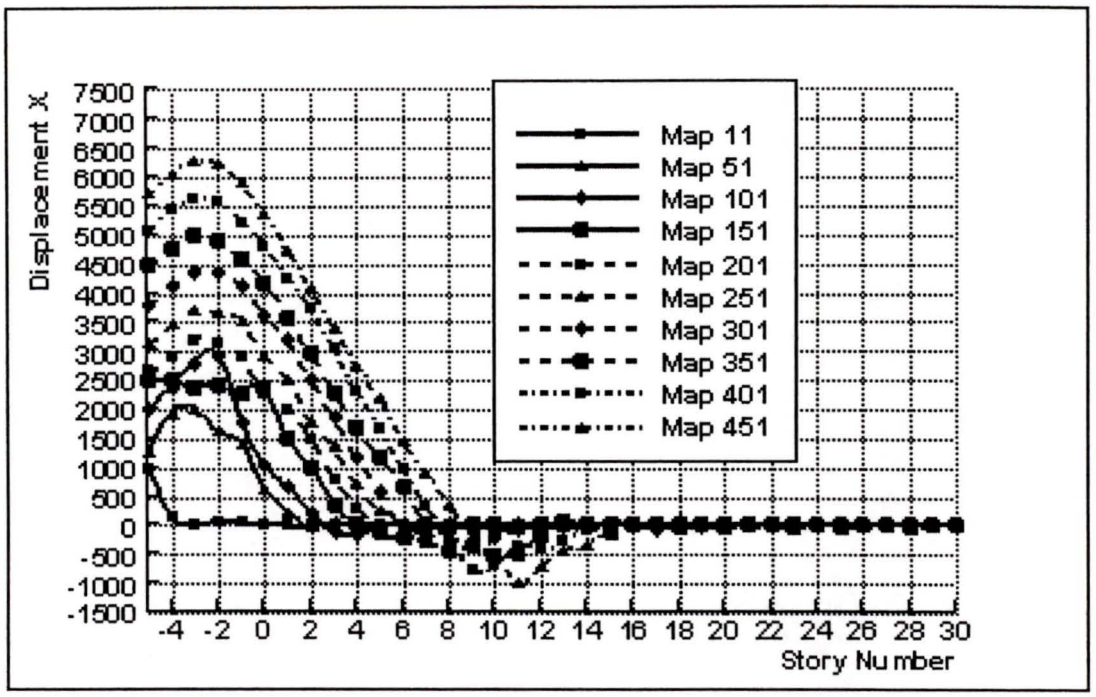

Figure 4.14 X direction displacement of the building at sampled time stations.

4.5 Stress Propagation on the Soil-Structure Interface

4.5.1 Notes on Stress Output Codes

The stress output codes in DSSIA are modified for matching the requirement by using the Tecplot software as the post-processing tool. The stress is stored in the output *file-name.NSO*. All the modifications are marked with author identity and date for consistent maintenance. The manual for the Tecplot gives detailed procedure and programming guides.

4.5.2 Normal Stress on the Side Wall

The stress on the side wall is illustrated in Figures 4.15-4.20. The figure show the normal stress concentration and the evolution of the stress on the side wall developed from the convergence around the surface to the middle depth of the basements. The stress first depends on the wave striking the building directly, and is then determined by the free vibration of the building.

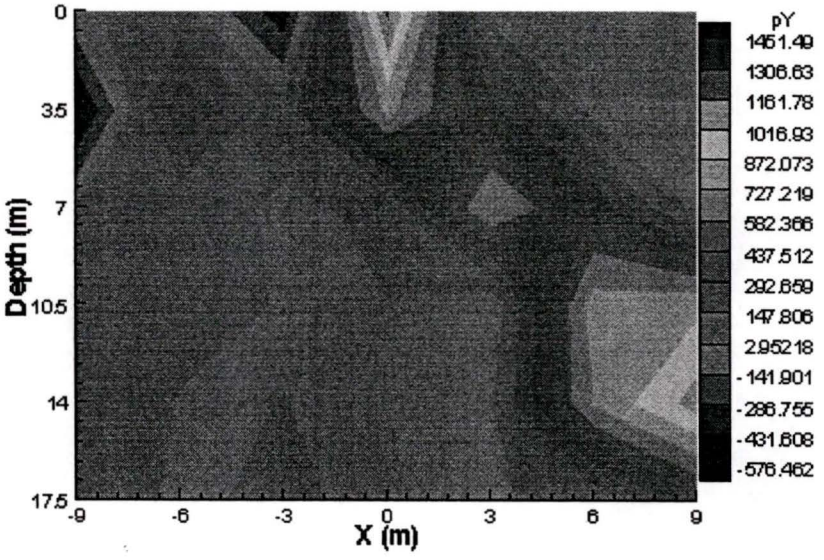

Figure 4.15 Normal stress on the side wall at 0.10s.

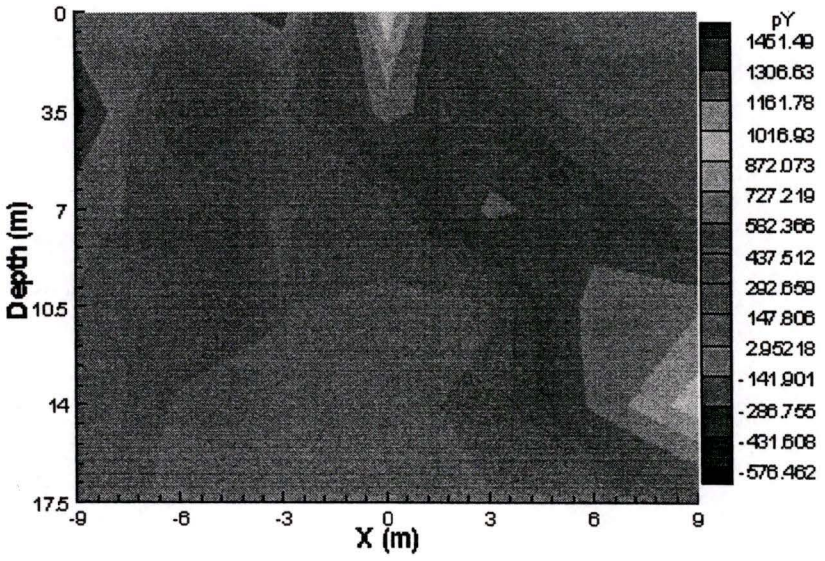

Figure 4.16 Normal stress on the side wall at 0.50s.

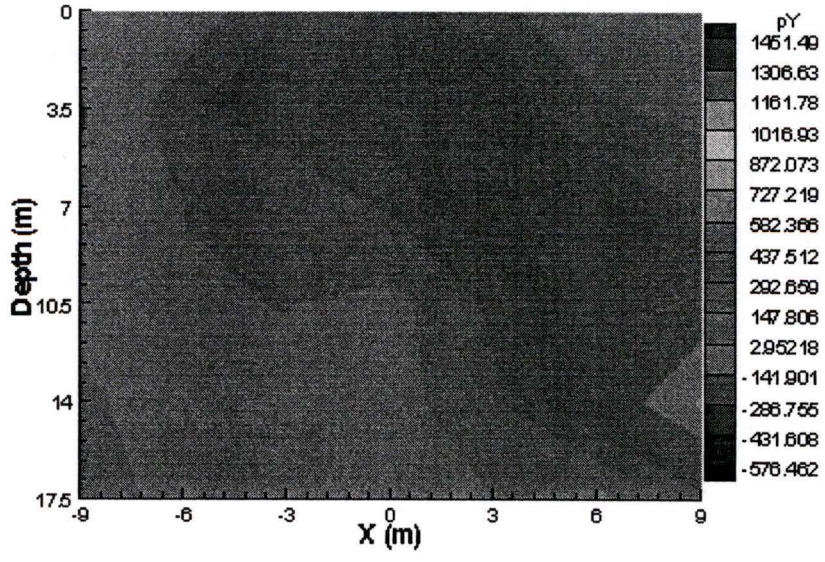

Figure 4.17 Normal stress on the side wall at 1.00s.

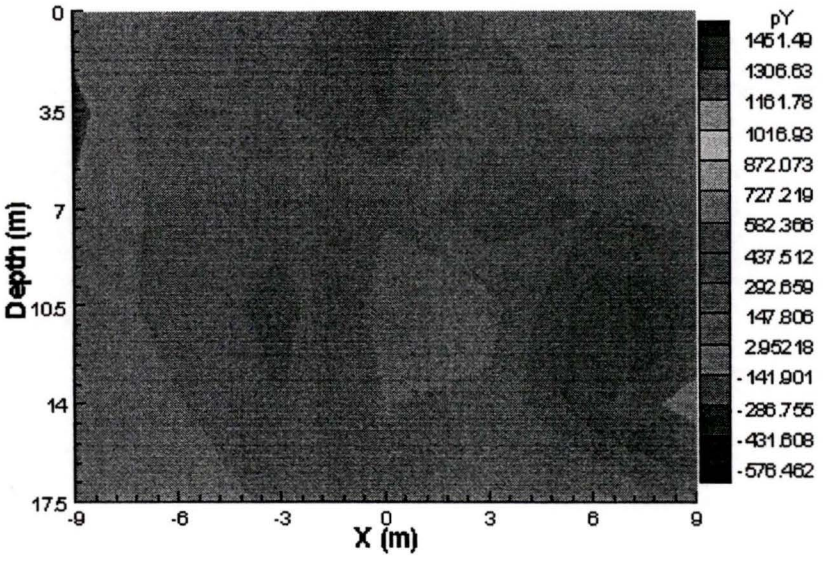

Figure 4.18 Normal stress on the side wall at 5.00s.

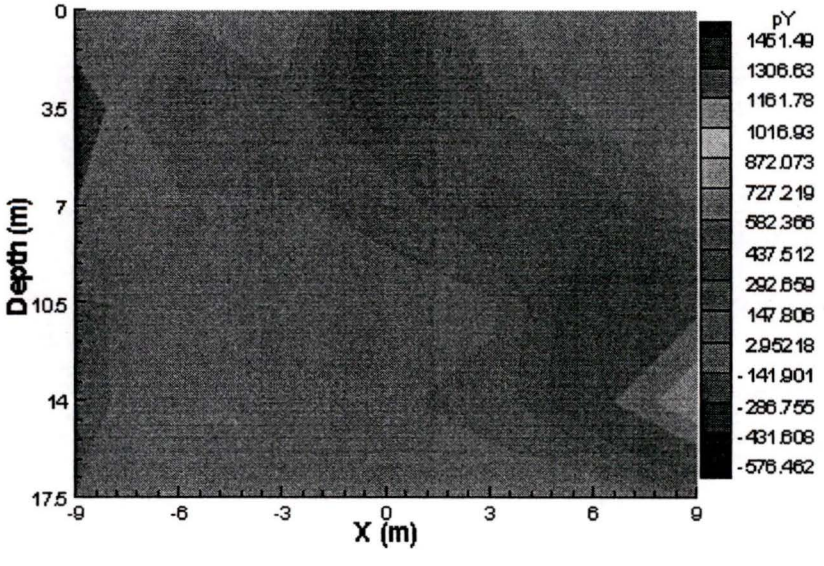

Figure 4.19 Normal stress on the side wall at 20.00s.

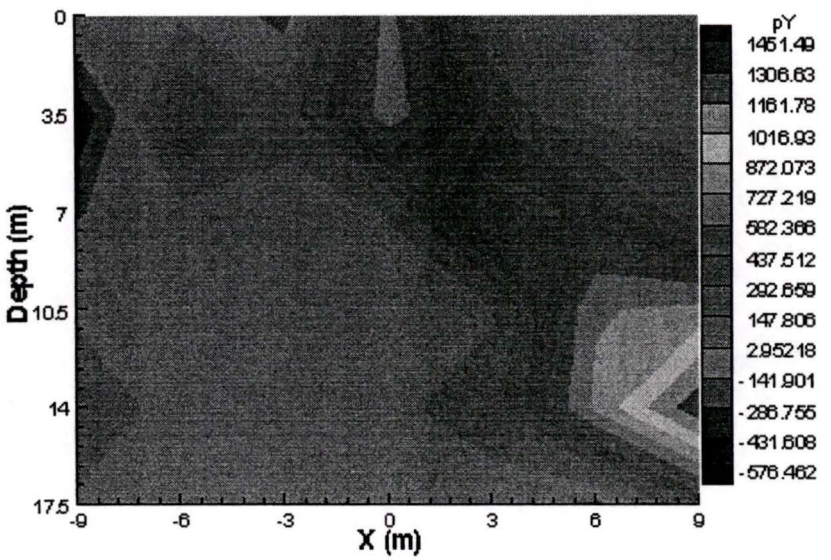

Figure 4.20 Normal stress on the side wall at 50.00s.

4.5.3 Normal Stress on the Front Wall

Since the front wall is perpendicular to the input plane X-Z and is symmetrical to the X-Z plane, the normal stress is therefore symmetrical to the center line (Figure 4.21-4.26). The normal stress propagation is presented in the series of diagrams. By checking the input Tabas data, the maximum acceleration is around 10~11 seconds in the time interval of 50 seconds. Also, the large amplitude of the acceleration occurs between 4 and 25 seconds. This leads the maximum stress to occur almost as the first wave strikes, and then the stress is quickly reduced. There are two symmetrical stress convergence sources close to the surface, which match the side wall maximum stress distribution. The concentration is

developed at both sides and close to the bottom, which matches the stress concentration of the side wall.

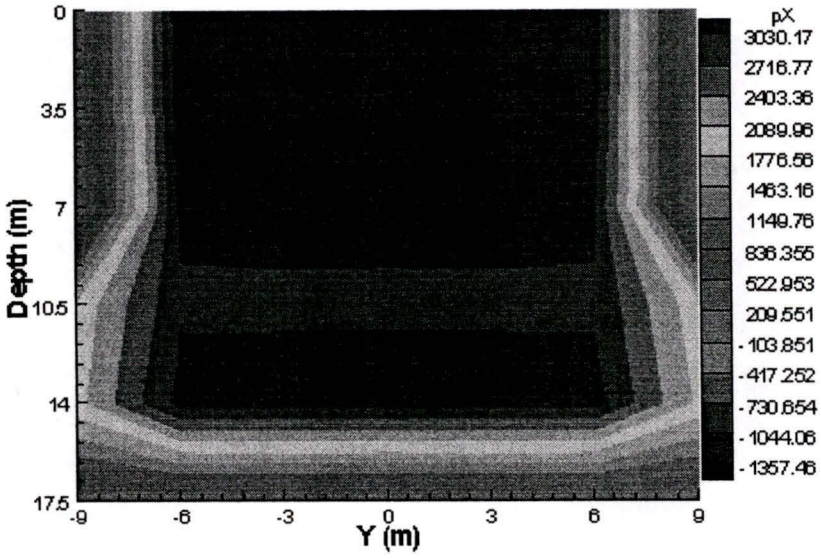

Figure 4.21 Normal stress on the front wall at 0.10s.

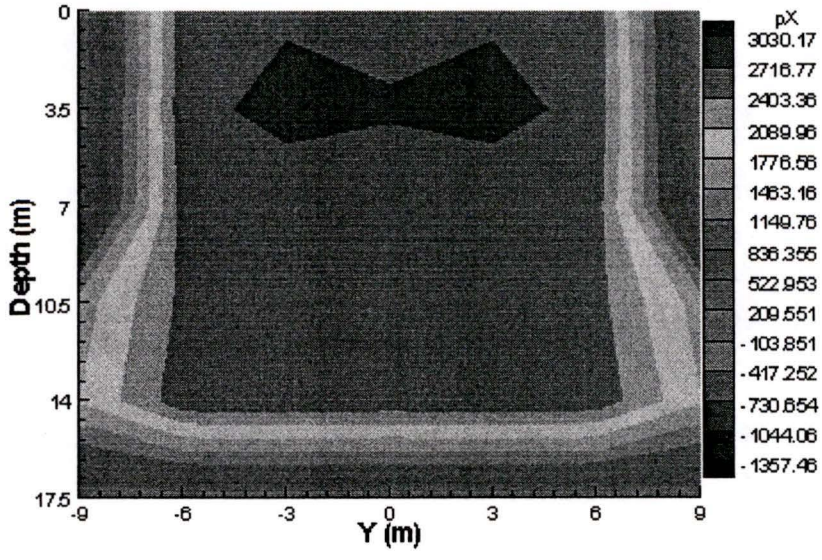

Figure 4.22 Normal stress on the front wall at 0.50s.

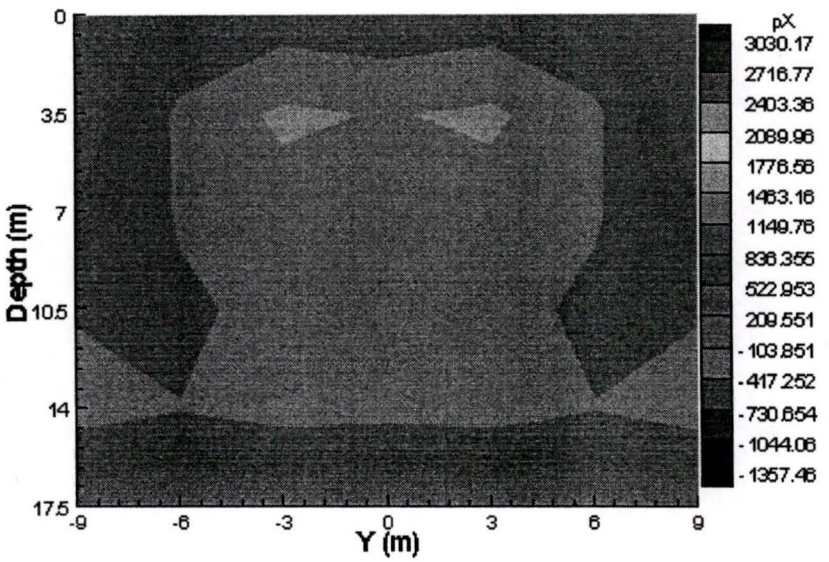

Figure 4.23 Normal stress on the front wall at 1.00s.

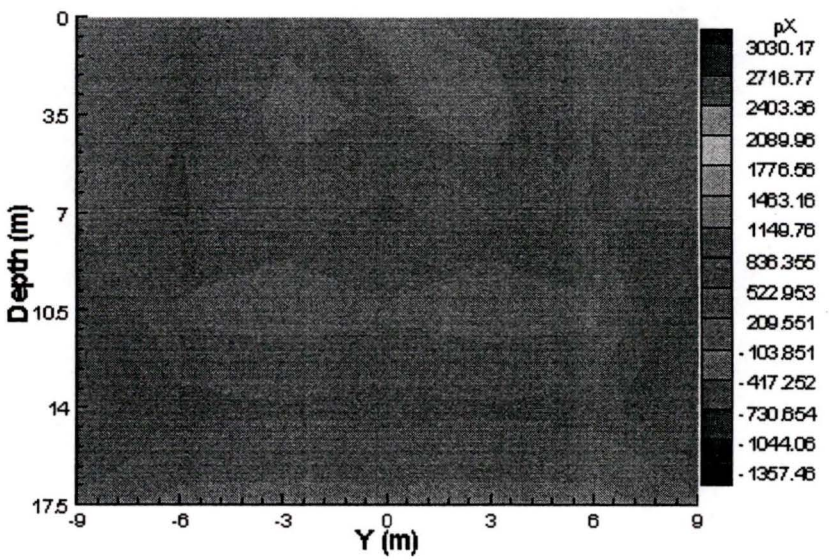

Figure 4.24 Normal stress on the front wall at 5.00s.

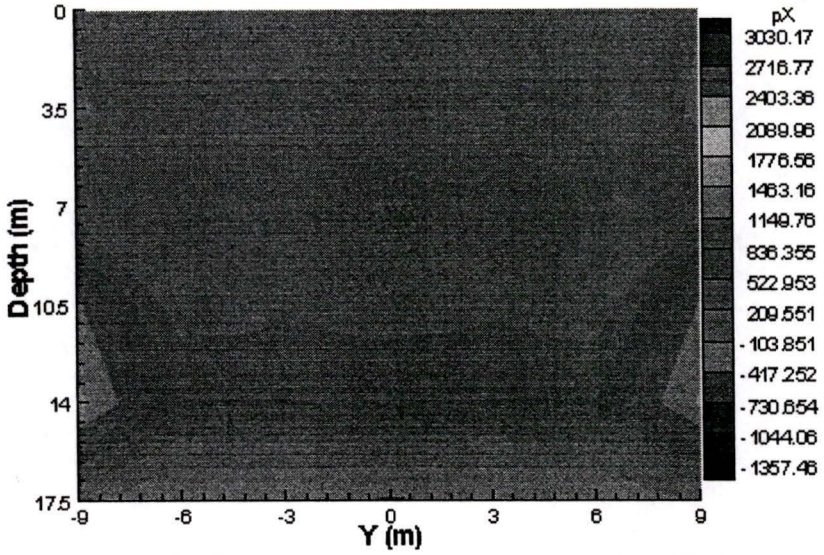

Figure 4.25 Normal stress on the front wall at 20.00s.

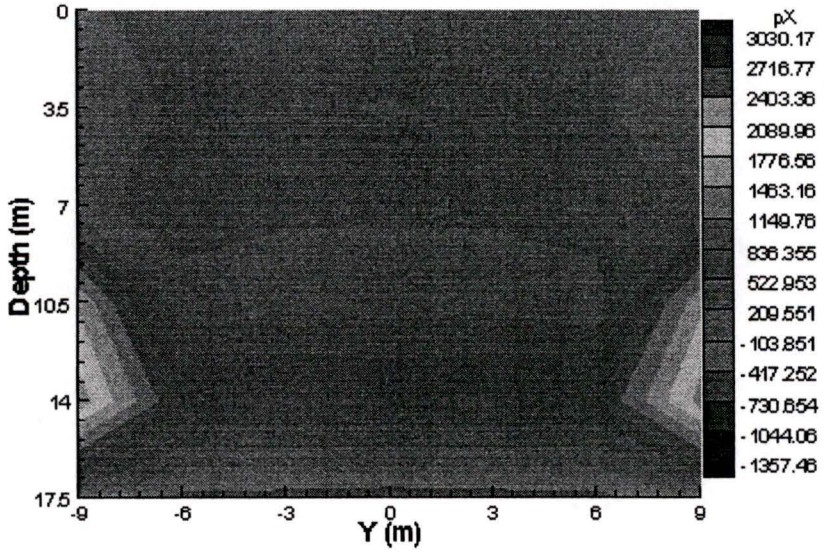

4.26 Normal stress on the front wall at 50.00s.

4.6 Conclusions from the Time Domain Analysis

Based on a new numerical procedure for solving the soil-structure interaction problem, we investigated the response of four different height buildings. The peak displacement of the nodes on the centerlines of the buildings are obtained and compared by considering the SSI effect and the geometrical factors after simulating a severe ground motion by using the Tabas earthquake recordings. The largest deformation of the building occurs in the basement level close to the free surface. The P waves cause more deformation and movement along the input direction, while the shear waves cause much more inter-story drifting which is vertical to the input direction. Finally, the time history of the displacement shows the buildings' dynamic vibration behavior.

By using this procedure, we are looking forward to simulating the response of underground lifelines and structures in civil engineering, communication and petroleum industry.

.

Chapter 5

Summary and Outlook

In this research work, the SSI effect on the tall building vibration is investigated for both frequency and time domains. The fundamental frequency, radiation damping ratio, dynamic response and stress propagation on the interface are provided. There are some questions left in modeling the unbounded soil, complex structure, and soil-structure interactions due to unknown properties, soil-dynamics and dynamical coupling. Further experiments on soil dynamic properties and building vibration elements will help to increase the accuracy of the numerical model. And the improvement in computing hardware and numerical algorithms will increase both the accuracy and confidence of the results. The contact problem of the soil and structure is another direction for a detailed understanding of the mechanism of the soil-structure interaction, such as support soil yielding, gap developing, slipping and uplifting. A study is helpful for designing new earthquake resistant structures for reducing damage. Finally the numerical approximation

method is becoming as important as analytical and experimental methods in engineering practice.

References

[1] Aki, K. and Richards P. G., *Quantitative seismology: theory and methods*, W. H. Freeman and Company, San Francisco, California. 1980.

[2] Alyagshi Eilouch, M. N. and Sandhu, R. S., A mixed method for transient analysis of soil-structure interaction under SH-motion, *Earthquake Engineering and Structural Dynamics* 14: 499-516, 1986.

[3] Arnold, D. Kerr, Sibaie, El. And Magdy, A., Validation of new equations for dynamic analysis of tall frame-type structures, *Earthquake Engineering and Structural Dynamics* 15: 549-563, 1987.

[4] Bathe, Klaus-Jurgen, Finite element procedures, Prentice-Hall, Inc. Englewood Cliffs, New Jersey. 1996.

[5] Brownjohn, Mark William, Pan, Tso Chien, and Deng, X. Y., Correlating dynamic characteristics form field measurements and numerical analysis of a high-rise building, *Earthquake Engineering and Structural Dynamics* 29: 523-543, 2000.

[6] Bryan Stafford-Smith, E. C., Estimating periods of vibration of tall buildings, *Journal of Structural Engineering*112: 1005-1019, 1986.

[7] Capuani, D., Klein, R., Antes, H., and Tralli, A., Dynamic soil-structure interaction of coupled shear walls by boundary element method, *Earthquake Engineering and Structural Dynamics* 24: 861-879, 1995.

[8] Chajes, Michael, J., Zhang, L., and Kirby, James, T., Dynamic analysis of tall building using reduced-order continuum model, *Journal of Structural Engineering* 122: 1284-1291, 1996.

[9] Chapel, F., Boundary element method applied to linear soil-structure interaction on a heterogeneous soil, *Earthquake Engineering and Structural Dynamics* 15: 815-829, 1987.

[10] Darbre, G. R. and Wolf, J. P., Criterion of stability and implementation issues of hybrid frequency-time-domain procedure for non-linear dynamic analysis, *Earthquake Engineering and Structural Dynamics* 16: 569-581, 1988.

[11] Eshraghi, H., Dravinski, M., Scattering of plane harmonic SH, SV, P and Rayleigh waves by non-axisymmetric three-dimensional canyons: a wave function expansion approach. *Earthquake Engineering and Structural Dynamics* 18: 983-998, 1989.

[12] Fukui, T., Time marching BE-FE method in 2-D elastodynamic problem, *International conference on BEM IX* Stuttgart, 1987.

[13] Goldberg ,John E., Bogdanoff, John L., and Moh, Za Lee, Forced vibration and natural frequencies of tall building frames, *Bulletin of the Seismological Society of America* 49: 33-47, 1959.

[14] Hart, Gary C. and Wong K. Structural Dynamics for Structural Engineers, John Wiley & Sons, 1999.

[15] Hassan Abouseeda, and Dakoulas Panos, Non-linear dynamic earth dam-foundation interaction using BE-FE method. *Earthquake engineering and structural dynamics* 27: 917-936, 1998.

[16] Housener, G.W. and Brady, A. G., Natural periods of vibration of buildings, *Journal of Engineering Mechanics Division Proceedings of the American Society of Civil Engineers* August: 31-65,1963.

[17] Israil, A. S. M. and Banerjee, P. K., Effects of geometrical and material properties on the vertical vibration of 3-D foundations by BEM, *International Journal Numerical Analysis Methods in Geomechanics* 14: 49-70, 1990.

[18] Jacobsen, Lydik S., Natural periods of uniform cantilever beams, *American Society of Civil Engineers Transactions* (Paper No. 2025): 402-431, 1933.

[19] Jennings, Paul C. and Skattum, K. S., Dynamic properties of planar coupled shear walls, *Earthquake Engineering and Structural Dynamics* 1 (4): 387-405, 1973.

[20] Kanai Kiyoshi and Yoshizawa Shizuyo, On the period and the damping of vibration of actual buildings *Bulletin of the Earthquake Research Institute* 39: 477-489, 1961.

[21] Kanok-Nukulchai, W. L., Sek Yean, and Karasudhi, Pisidhi, A versatile finite strip model for three-dimensional tall building analysis, *Earthquake engineering and structural dynamics* 11 (2): 149-166, 1983.

[22] Karabalis, D. L. and Beskos, D. E., Dynamic response of 3-D flexible foundations by time domain BEM and FEM, *Soil Dynamics and Earthquake Engineering* 4: 91-101, 1985

[23] Kausel, E., Local transmitting boundaries, *Journal of Engineering Mechanics, ASCE* 114: 1011-1027, 1988.

[24] Kausel, E., Rosset, J. M., and Wass, G., Dynamic analysis of footings on layered media, *Journal of Engineering Mechanics, ASCE* 101: 679-693, 1975.

[25] Kawakami, H., Rocking compliance functions for rigid bases allowed to uplift, *Journal of Geotechnical Engineering* 116: 725-739, 1990.

[26]Lambros S. Katafygiotis, C. P. , Dynamic response variability of structures with uncertain properties, *Earthquake engineering and structural dynamics* **25**(8): 775-793,1996.

[27] Li, Q. S., Fang, J. Q., Jeary, A. P., Wong, C. K., and Liu, D. K., Evaluation of wind effects on a supertall building based on full-scale measurements, *Earthquake Engineering and Structural Dynamics* 29**:** 1845-1862, 2000.

[28] Luco, J. E., Soil-structure interaction and identification of structural models, Proceedings of the 2nd ASCE Conference on Civil Engineering and Nuclear Power, Vol 2: 10/1/1-10/1/31, 1980.

[29] MeCallen, D.B. and Romastad, K. M., Nonlinear model for building-soil systems, *Journal of Engineering Mechanics* 120 (5): 1129-1152, 1992.

[30] Nagashima, I. M., R., Asami, Y., Hirai, J., and Abiru, H., Performance of hybrid mass damper system applied to a 36-story high-rise building, *Earthquake Engineering and Structural Dynamics* 30 (11): 1615-1637, 2001.

[31] Nakamura, Y., Tanaka, K., Nakayama, M., and Fujita, T., Hybrid mass dampers using two types of electric servomotors: AC servomotors and linear-induction servomotors, *Earthquake Engineering and Structural Dynamics* 30 (11): 1719-1743, 2001.

[32] Nielsen, S. R. K., Merk, K. J., and Thoft-Christensen P., Response analysis of hysteretic multi-story frames under earthquake excitation, *Earthquake Engineering and Structural Dynamics* 18: 655-666, 1989.

[33] Psycharis, I. N. and Jennings, P.C., Rocking of slender rigid bodies allowed to uplift. *Earthquake engineering and Structural Dynamics* 11: 57-76, 1983.

[34] Rodriguez, Mario E. and Montes, Roberto, Seismic response and damage analysis of buildings supported of flexible soils, *Earthquake Engineering and Structural Dynamics* 29: 647-665, 2000.

[35] Rucker, W., Dynamic behaviour of rigid foundations of arbitrary shape on a half-space, *Earthquake Engineering and Structural Dynamics* 10: 675-690, 1982.

[36] Safak E., Detection and identification of soil-structure interaction in buildings from vibration recordings, *Journal of Structural Engineering*, 121: 899-906, 1995.

[37] Saito, T., Shiba, K., and Tamura K., Vibration control characteristics of a hybrid mass damper system installed in tall buildings, *Earthquake Engineering and Structural Dynamics* 30: 1677-1696, 2001.

[38] Sanchez-Sesma, Francisco, J., Diffraction of elastic waves by three-dimensional surface irregularities, *Bulletin of the Seismological Society of America* 73 (6): 1621-1636, 1983.

[39] Sarma, S. K. and Srbulov, M., A simplified method for prediction of kinematic soil-foundation interaction effects on peak horizontal acceleration of a rigid foundation, *Earthquake Engineering and Structural Dynamics* 25 (8): 815-836: 1996.

[40] Song, C. and Wolf, J. P. Consistent infinitesimal finite-element cell method: three-dimensional vector wave equation, *International Journal for Numerical Methods in Engineering* 39: 2189-2208, 1996.

[41] Spyrakos, C. C. and Beskos, D. E., Dynamic response of flexible strip foundations by boundary and finite elements, *Soil Dynamics and Earthquake Engineering* 5: 84-96, 1986.

[42] Stewart, Jonathan P. and Fenves, Gregory L., System identification for evaluating soil-structure interaction effects in buildings from strong motion recordings, *Earthquake Engineering and Structural Dynamics* 27: 869-885, 1998.

[43] Takemori, T., Sotomura, K. and Yamada, M., Nonlinear dynamic response of reactor containment, *Nuclear Engineering and Design* 38: 463-474, 1976.

[44] Takeuchi, H. and Saito, M., *Seismic surface waves, in Methods in computational physics*, vol. 11, B. A. Bolt, Editor, Academic Press, New York. 1972.

[45] Tehranizadeh, M. Soil-structure interaction of tall building, *Proceedings 11th European Conference on Earthquake Engineering, Paris,6 -11 September 1998.* Rotterdam: Balkema, 1998.

[46] Toki, K. and Fu, C. S., Generalized method for non-linear seismic response analysis of a three dimensional soil-structure interaction system, *Earthquake Engineering and Structural Dynamics* 15: 945-961, 1987.

[47] Von Estorff O. and Kausel E., Coupling of boundary and finite elements for soil-structure interaction problems, *Earthquake Engineering and Structural Dynamics* 18 (7): 1065-1075, 1989.

[48] Von Estorff O. and Prabucki, M.J., The coupling of boundary and finite elements to solve transient problems in elastodynamics, P. 447-450. Boundary Elements X, vol. 4. Edited by Brebbia, C. A., Heidelberg, New York, Springer Verlag, 1988.

[49] Wass, G., Linear tow-dimensional analysis of soil dynamics problems in semi-infinete layered media, *Ph.D. thesis*, University of California, Berkeley, CA. 1972.

[50] Wegner J. L. and Zhang X., Free-vibration analysis of a three-dimensional soil-structure system, *Earthquake Engineering and Structural Dynamics* 30: 43-57, 2001.

[51] Whitman, R. V. and Richart, F. E. Jr., Design procedures for dynamically loaded Foundations, *Journal of the Soil Mechanics and Foundations Division*, ASCE, Vol. 93. No. SM6: 169-193, 1967.

[52] Wolf, J.P., Soil-structure interaction with separation of base mat from soil (lifting-off), *Nuclear Engineering and Design* 38 (2): 357-384, 1976.

[53] Wolf, J. P., *Dynamic soil-structure interaction*, Prentice-Hall, Englewood Cliffs, N.J., 1985.

[54] Wolf, J.P., *Soil-Structure-Interaction Analysis in Time Domain,* Englewood Cliffs: Prentice-Hall, 1988.

[55] Wolf, J. P., Spring-dashpot-mass model for foundation vibrations, *Earthquake Engineering and Structural Dynamics* 26: 931-949, 1997.

[56] Wolf, J. P. and Darbre, Georges R., Non-linear soil-structure interaction analysis based on the boundary-element method in time domain with application to embedded foundation, *Earthquake Engineering and Structural Dynamics* 14: 83-101, 1986.

[57] Wolf, J. P. and Obernhuber, P., Non-linear soil-structure-interaction analysis using dynamic stiffness or flexibility of soil in the time domain, *Earthquake Engineering and Structural Dynamics* 13: 195-212, 1985a.

[58] Wolf, J. P. and Obernhuber, P., Non-linear soil-structure-interaction analysis using Green's function of soil in the time domain, *Earthquake Engineering and Structural Dynamics* 13: 213-223, 1985b.

[59] Wolf, J. P. and Skrikerud, P.E., Seismic excitation with large overturning moments: tensile capacity, projecting base mat or lifting-off, *Nuclear Engineering and Design* 50: 305-321, 1978.

[60] Wolf, J.P. and Song, C. *Finite-element modelling of unbounded media,* Chichester: Wiley, 1996.

[61] Wolf, J. P., and Song, C. The scaled boundary finite-element method-alias consistent infinitesimal finite-element method-for elastodynamics, *Computer Methods in Applied Mechanics and Engineering* 147: 329-355, 1997.

[62] Wu, W. H., Wang, J. F., and Lin, C. C., Systematic assessment of irregular building-soil interaction using efficient modal analysis, *Earthquake engineering and structural dynamics* 30: 573-594, 2001.

[63] Zhang Chuhan, Chen Xinfeng, and Wang Guanglun, A coupling model of FE-BE-IE-IBE for non-linear layered soil-structure interactions, *Earthquake engineering and structural dynamics* 28: 421-441, 1999.

[64] Zhang, X., Wegner, J. L., and Haddow, J. B., SSWIA-3D, a three-dimensional soil-structure-wave interaction analysis program (Unpublished manual), Department of Mechanical Engineering, University of Victoria, July, 1998.

[65] Zhang X., Wegner, J.L., and Haddow J. B., Three-dimensional dynamic soil-structure interaction analysis in the time domain, *Earthquake Engineering and Structural Dynamics* 28: 1501-1524, 1999.

[66] Yao M. M., Wegner J. L., and Zhang X., Dynamic soil-structure-wave interaction of a tall building, Structural Dynamics, EURDYN2002, Grundmann & Schueller (eds), Swets & Zeitlinger, Lisse, 2002. ".

Appendix A

Definitions for Soil-Structure Interaction System

Shear-wall building: the relative displacement between floors is horizontal, and the shear force in a story only depends on the relative displacement of the two floors and is independent of the displacements in adjoining stories. This definition is based on the nature of the deformation rather than on the means for attaching it. Typical multistory office building with masonry walls appear to be the shear-wall type even though the walls have many window openings, and partition walls, stairways etc., participating in the structural action.

Frame building: the skeleton of the building is made of a steel frame and is the main support of the building weight and dynamic load. Modern tall buildings usually adopt this structure for the high strength, light weight and high flexibility, compared with a masonry material. In this thesis, the superstructure is a frame structure.

Foundation: is the support of the superstructure and basement in the form of a thicker reinforced steel concrete mat. Some mats are connected with a group of reinforced concrete piles to provide further resistance to overturning of the tall building. In this thesis, with the assumption of the weld condition between the foundation and the underneath soil, the foundation is assigned the same thickness and material as the basement-wall.

Superstructure: is the portion of the building above the ground.

Basement: is the portion of the building under the ground. This part is usually used for parking, storage, or as a mechanical room.

Soil: the soil is a mixture of solid particles, water, and air. Usually the air is ignored. The water content is influenced by the underground water table depth. Above the water line, the soil is assumed to be drained soil. Below the water line, the soil is dealt as undrained soil. With the increase of the depth of the soil, the hydrostatic pressure also increases. When there is wave propagation, the stress in the soil shall include the hydrodynamic components in the effective stress of the soil. Due to the complexity of the soil and the size of this research subject, the soil's dynamic characteristic is not an intense concern in the thesis. A further advance of the research presented in this thesis will be to include a more complex constitutive equation for the soil than that of a linear elastic solid which was used in this thesis.

Unbounded soil: to model the unbounded soil mathematically, the soil is assumed to occupy an infinite space or semi-infinite space. Subject to wave propagation, the radiation condition must be satisfied in the solution of the governing equation of the soil-structure system. In order to model the unbounded media properly, the scaled boundary finite elements are employed and the radiation condition is satisfied when the thickness of the finite element cell approaches zero.

Structure: the whole building including the superstructure, basement and foundation.

Soil-structure interface: there is no actual interface between the soil and wall of the basement. In this thesis, the soil and structure are assumed to be welded together. So there is an interface coinciding with the wall.

Appendix B

Formulas for Elastodynamics

In a homogeneous isotropic body, the displacement satisfies three field equations. The displacement field is represented using tensor u_i. The subscript i represents the i-th component direction of deformation, and $i = 1,2,3$ for 3-dimensional problem. The equation of motion is given for a cubic body with unit volume,

$$\sigma_{ij,j} + b_i = \rho \ddot{u}_i \tag{1}$$

Where $\sigma_{ij,j}$ represents stresses increment along i-th direction, the b_i represents the i-th direction body force, and $\rho \ddot{u}_i$ is the term of initial force due to the i-th direction acceleration $\ddot{u}_i$ on the body with density ρ. The upper dot means the derivative to time. This is the fundamental equation for elastodynamics.

The relationship between the stress and strain is given using Hooke's law,

$$\sigma_{ij} = \lambda \varepsilon_{kk} \delta_{ij} + 2\mu \varepsilon_{ij} \tag{2}$$

where δ_{ij} is the Delta function, (if i=j, δ_{ij}=1; else, zero), ε_{ij} is the strain, λ and μ are Lamé constants.

Further the strain will be given in form of displacement using the relationship,

$$\varepsilon_{ij} = (u_{i,j} + u_{j,i})/2 \tag{3}$$

Substitute equation (3) into Hooke's law and the result in turn substitute into (1) to get the governing equation,

$$\mu u_{i,jj} + (\lambda + \mu) u_{j,ji} + b_i = \rho \ddot{u}_i \tag{4}$$

The Lamé constants λ and μ can be represented by the Young's modulus E and Possion's ratio ν, which are usually given in engineering measurements.

$$\lambda = E\nu/[(1+\nu)(1-2\nu)] \tag{5}$$

$$\mu = 0.5E/(1+\nu) \tag{6}$$

With the initial and boundary condition, the displacement field can be given by above equations.

The governing equation (4) is transformed to curvilinear coordinates, which are located at the soil-structure interface, in the scaled boundary finite element method. The scaling center is the apex of the truncated pyramid and also the reference point of the position vector. The unbounded soil is approximated as one linear elastic isotropic material.

Appendix C

Input Data

This an example for a 30 story building with 5 level-basement subject to Tabas earthquake strong motion in P wave at 30 degree input angle.

```
1764    1    3    0    1  499   1.0E-01      0.00    0    0
   20   20    6    0    0    0   1.0E-02
    0    3   4.0E+02   1.0E-01   1.0E-03   1.0E-03   0.1E-01   4.0E+01
    0    0    0    1
    2    0    0
    1       0.0       0.0
    1    0    0    0    1
    1    1    0
    1  501
    1  501
    0.0000     0.0000     0.1       13.27       0.2         4.9154     0.3
15.0249
    0.4       14.7871     0.5       10.1399     0.6         2.5923     0.7
6.6079
    0.8      -15.3866     0.9      -12.8535     1.00        0.2163     1.1
4.2527
    1.2       -8.1128     1.3      -13.6285     1.4       -12.6877     1.5
0.4957
    1.6       -3.5083     1.7       -9.4932     1.8        -5.7869     1.9
5.8461
    2.00     -19.2312     2.1       10.9993     2.2        -3.3265     2.3
-27.4839
    2.4      -13.0093     2.5      -11.6998     2.6        27.6533     2.7
30.0035
    2.8      -66.0589     2.9      -10.4762     3.00       14.383      3.1
27.8453
    3.2       -2.7544     3.3      -19.5377     3.4        -2.0986     3.5
13.6587
    3.6      -34.3623     3.7      -15.0988     3.8        -5.5579     3.9
-29.0871
    4.00     -52.7237     4.1      -11.1325     4.2       -20.7561     4.3
-57.4619
    4.4       78.7765     4.5      170.871      4.6       225.281      4.7
141.671
    4.8     -99.1951    4.9    -145.144     5.00   -120.351

....
....
....

   44          0.0       44.1       10.6286    44.2         9.191     44.3
0.5933
   44.4        5.2398     44.5        5.4737    44.6         1.9812    44.7
20.8575
   44.8       12.8568     44.9        5.2495    45           0.3925    45.1
13.5886
   45.2        2.3606     45.3       15.5639    45.4        -5.5653    45.5
1.6606
   45.6      -32.9986     45.7      -24.8812    45.8        13.6519    45.9
-15.009
   46        -19.1386     46.1      -13.7476    46.2        -0.6005    46.3
-23.6464
```

```
   46.4          8.3484    46.5         32.208     46.6        -11.6143    46.7
381.314
   46.8       -221.371     46.9        -47.0963    47            3.7822    47.1
-50.1027
   47.2        -11.6694    47.3         25.9901    47.4         71.8994    47.5
-39.2347
   47.6         -7.4364    47.7         27.7134    47.8         -2.658     47.9
0.2376
   48           -7.6453    48.1        -17.6756    48.2         15.274     48.3
-36.0302
   48.4        -20.225     48.5         -1.855     48.6          4.658     48.7
11.4784
   48.8         10.2682    48.9          1.2237    49          -26.8345    49.1
2.7974
   49.2        -23.273     49.3         -7.7346    49.4         -0.9121    49.5
-10.9472
   49.6         11.0143    49.7          5.7198    49.8          0.5393    49.9
6.5582
   50           0.0
    1    0    0    0    0    0    0    -9.000    -9.000     0.000
    2    0    0    0    0    0    0    -6.000    -9.000     0.000
    3    0    0    0    0    0    0    -3.000    -9.000     0.000
    4    0    0    0    0    0    0     0.000    -9.000     0.000
    5    0    0    0    0    0    0     3.000    -9.000     0.000
    6    0    0    0    0    0    0     6.000    -9.000     0.000
    7    0    0    0    0    0    0     9.000    -9.000     0.000
    8    0    0    0    0    0    0    -9.000    -6.000     0.000
    9    0    0    0    0    0    0     9.000    -6.000     0.000
   10    0    0    0    0    0    0    -9.000    -3.000     0.000
   11    0    0    0    0    0    0     9.000    -3.000     0.000
   12    0    0    0    0    0    0    -9.000     0.000     0.000
   13    0    0    0    0    0    0     9.000     0.000     0.000
   14    0    0    0    0    0    0    -9.000     3.000     0.000
   15    0    0    0    0    0    0     9.000     3.000     0.000
   16    0    0    0    0    0    0    -9.000     6.000     0.000
   17    0    0    0    0    0    0     9.000     6.000     0.000
   18    0    0    0    0    0    0    -9.000     9.000     0.000
   19    0    0    0    0    0    0    -6.000     9.000     0.000
   20    0    0    0    0    0    0    -3.000     9.000     0.000
   21    0    0    0    0    0    0     0.000     9.000     0.000
   22    0    0    0    0    0    0     3.000     9.000     0.000
   23    0    0    0    0    0    0     6.000     9.000     0.000
   24    0    0    0    0    0    0     9.000     9.000     0.000
   25    0    0    0    0    0    0    -9.000    -9.000     3.500
   26    0    0    0    0    0    0    -6.000    -9.000     3.500
   27    0    0    0    0    0    0    -3.000    -9.000     3.500
   28    0    0    0    0    0    0     0.000    -9.000     3.500
   29    0    0    0    0    0    0     3.000    -9.000     3.500
   30    0    0    0    0    0    0     6.000    -9.000     3.500
   31    0    0    0    0    0    0     9.000    -9.000     3.500
   32    0    0    0    0    0    0    -9.000    -6.000     3.500
   33    0    0    0    0    0    0     9.000    -6.000     3.500
   34    0    0    0    0    0    0    -9.000    -3.000     3.500
   35    0    0    0    0    0    0     9.000    -3.000     3.500
   36    0    0    0    0    0    0    -9.000     0.000     3.500
   37    0    0    0    0    0    0     9.000     0.000     3.500
   38    0    0    0    0    0    0    -9.000     3.000     3.500
   39    0    0    0    0    0    0     9.000     3.000     3.500
   40    0    0    0    0    0    0    -9.000     6.000     3.500
   41    0    0    0    0    0    0     9.000     6.000     3.500
```

```
   42    0    0    0    0    0    0    -9.000     9.000     3.500
   43    0    0    0    0    0    0    -6.000     9.000     3.500
   44    0    0    0    0    0    0    -3.000     9.000     3.500
   45    0    0    0    0    0    0     0.000     9.000     3.500
   46    0    0    0    0    0    0     3.000     9.000     3.500
   47    0    0    0    0    0    0     6.000     9.000     3.500
   48    0    0    0    0    0    0     9.000     9.000     3.500
....
....
....
  153    0    0    0    0    0    0     3.000    -3.000    17.500
  154    0    0    0    0    0    0     6.000    -3.000    17.500
  155    0    0    0    0    0    0    -6.000     0.000    17.500
  156    0    0    0    0    0    0    -3.000     0.000    17.500
  157    0    0    0    0    0    0     0.000     0.000    17.500
  158    0    0    0    0    0    0     3.000     0.000    17.500
  159    0    0    0    0    0    0     6.000     0.000    17.500
  160    0    0    0    0    0    0    -6.000     3.000    17.500
  161    0    0    0    0    0    0    -3.000     3.000    17.500
  162    0    0    0    0    0    0     0.000     3.000    17.500
  163    0    0    0    0    0    0     3.000     3.000    17.500
  164    0    0    0    0    0    0     6.000     3.000    17.500
  165    0    0    0    0    0    0    -6.000     6.000    17.500
  166    0    0    0    0    0    0    -3.000     6.000    17.500
  167    0    0    0    0    0    0     0.000     6.000    17.500
  168    0    0    0    0    0    0     3.000     6.000    17.500
  169    0    0    0    0    0    0     6.000     6.000    17.500
  170    0    0    0    1    1    1    -9.000    -9.000  -105.000
  171    0    0    0    1    1    1    -6.000    -9.000  -105.000
  172    0    0    0    1    1    1    -3.000    -9.000  -105.000
  173    0    0    0    1    1    1     0.000    -9.000  -105.000
  174    0    0    0    1    1    1     3.000    -9.000  -105.000
  175    0    0    0    1    1    1     6.000    -9.000  -105.000
  176    0    0    0    1    1    1     9.000    -9.000  -105.000
  177    0    0    0    1    1    1    -9.000    -6.000  -105.000
  178    0    0    0    1    1    1    -6.000    -6.000  -105.000
  179    0    0    0    1    1    1    -3.000    -6.000  -105.000
  180    0    0    0    1    1    1     0.000    -6.000  -105.000
  181    0    0    0    1    1    1     3.000    -6.000  -105.000
  182    0    0    0    1    1    1     6.000    -6.000  -105.000
  183    0    0    0    1    1    1     9.000    -6.000  -105.000
  184    0    0    0    1    1    1    -9.000    -3.000  -105.000
  185    0    0    0    1    1    1    -6.000    -3.000  -105.000
  186    0    0    0    1    1    1    -3.000    -3.000  -105.000
  187    0    0    0    1    1    1     0.000    -3.000  -105.000
  188    0    0    0    1    1    1     3.000    -3.000  -105.000
  189    0    0    0    1    1    1     6.000    -3.000  -105.000
  190    0    0    0    1    1    1     9.000    -3.000  -105.000
  191    0    0    0    1    1    1    -9.000     0.000  -105.000
  192    0    0    0    1    1    1    -6.000     0.000  -105.000
  193    0    0    0    1    1    1    -3.000     0.000  -105.000
  194    0    0    0    1    1    1     0.000     0.000  -105.000
  195    0    0    0    1    1    1     3.000     0.000  -105.000
  196    0    0    0    1    1    1     6.000     0.000  -105.000
  197    0    0    0    1    1    1     9.000     0.000  -105.000
  198    0    0    0    1    1    1    -9.000     3.000  -105.000
  199    0    0    0    1    1    1    -6.000     3.000  -105.000
  200    0    0    0    1    1    1    -3.000     3.000  -105.000
  201    0    0    0    1    1    1     0.000     3.000  -105.000
```

```
  202     0     0     0     1     1     1      3.000      3.000   -105.000
  203     0     0     0     1     1     1      6.000      3.000   -105.000
  204     0     0     0     1     1     1      9.000      3.000   -105.000
  205     0     0     0     1     1     1     -9.000      6.000   -105.000
  206     0     0     0     1     1     1     -6.000      6.000   -105.000
  207     0     0     0     1     1     1     -3.000      6.000   -105.000
  208     0     0     0     1     1     1      0.000      6.000   -105.000
  209     0     0     0     1     1     1      3.000      6.000   -105.000
  210     0     0     0     1     1     1      6.000      6.000   -105.000
  211     0     0     0     1     1     1      9.000      6.000   -105.000
  212     0     0     0     1     1     1     -9.000      9.000   -105.000
  213     0     0     0     1     1     1     -6.000      9.000   -105.000
  214     0     0     0     1     1     1     -3.000      9.000   -105.000
  215     0     0     0     1     1     1      0.000      9.000   -105.000

....
....
....
....

 1741     0     0     0     1     1     1     -3.000     -6.000     14.000
 1742     0     0     0     1     1     1      0.000     -6.000     14.000
 1743     0     0     0     1     1     1      3.000     -6.000     14.000
 1744     0     0     0     1     1     1      6.000     -6.000     14.000
 1745     0     0     0     1     1     1     -6.000     -3.000     14.000
 1746     0     0     0     1     1     1     -3.000     -3.000     14.000
 1747     0     0     0     1     1     1      0.000     -3.000     14.000
 1748     0     0     0     1     1     1      3.000     -3.000     14.000
 1749     0     0     0     1     1     1      6.000     -3.000     14.000
 1750     0     0     0     1     1     1     -6.000      0.000     14.000
 1751     0     0     0     1     1     1     -3.000      0.000     14.000
 1752     0     0     0     1     1     1      0.000      0.000     14.000
 1753     0     0     0     1     1     1      3.000      0.000     14.000
 1754     0     0     0     1     1     1      6.000      0.000     14.000
 1755     0     0     0     1     1     1     -6.000      3.000     14.000
 1756     0     0     0     1     1     1     -3.000      3.000     14.000
 1757     0     0     0     1     1     1      0.000      3.000     14.000
 1758     0     0     0     1     1     1      3.000      3.000     14.000
 1759     0     0     0     1     1     1      6.000      3.000     14.000
 1760     0     0     0     1     1     1     -6.000      6.000     14.000
 1761     0     0     0     1     1     1     -3.000      6.000     14.000
 1762     0     0     0     1     1     1      0.000      6.000     14.000
 1763     0     0     0     1     1     1      3.000      6.000     14.000
 1764     0     0     0     1     1     1      6.000      6.000     14.000
    0     0
   2  48   0   0   0   0   4   0   0   0   0   0   0   0   1   1   0   0
0   0
    1 1.000E+00
 2.500E+00 3.300E-01
    1     4     1
    1     2    26    25
    2     4     1
    2     3    27    26
    3     4     1
    3     4    28    27
    4     4     1
    4     5    29    28
....
....
....
```

```
   46    45    69    70
   47     4     1
   47    46    70    71
   48     4     1
   48    47    71    72
    2  72    0    0    0    0    4    0    0    0    0    0    0    0    1    2    0    0
0    0
    1 1.000E+00
 2.500E+00 3.000E-01
    2 1.000E+00
 2.500E+00 3.000E-01
    1     4     2
   49    50    74    73
    2     4     2
   50    51    75    74
    3     4     2
   51    52    76    75
    4     4     2
   52    53    77    76
    5     4     2
....
....
....

   66     4     2
  113   120   144   137
   67     4     2
  115   114   138   139
   68     4     2
  116   115   139   140
   69     4     2
  117   116   140   141
   70     4     2
  118   117   141   142
   71     4     2
  119   118   142   143
   72     4     2
  120   119   143   144
    2  36    0    0    0    0    4    0    0    0    0    0    0    0    1    3    0    0
0    0
    1 1.000E+00
 2.500E+00 3.000E-01
    2 1.000E+00
 2.500E+00 3.000E-01
    3 1.000E+00
 2.500E+00 3.000E-01
    1     4     3
  121   122   145   128
    2     4     3
  122   123   146   145
    3     4     3
  123   124   147   146
    4     4     3
  124   125   148   147
    5     4     3
  125   126   149   148

....
....
```

```
....

   33    4    3
  166  167  141  140
   34    4    3
  167  168  142  141
   35    4    3
  168  169  143  142
   36    4    3
  169  137  144  143
   31260   0   0   0   0   8   0   0   0   0   0   0   0   1   4   0   0
0   0
    1 1.000E+00
 2.500E+00 3.000E-01
    2 1.000E+00
 2.500E+00 3.000E-01
    3 1.000E+00
 2.500E+00 3.000E-01
    4 1.000E+00
 2.500E+00 3.000E-01
    1    8    8    0    4
  220  227  226  219  171  178  177  170

    2    8    8    0    4
  221  228  227  220  172  179  178  171

    3    8    8    0    4
  222  229  228  221  173  180  179  172

    4    8    8    0    4
  223  230  229  222  174  181  180  173

    5    8    8    0    4
  224  231  230  223  175  182  181  174

....
....
....

 1255    8    8    0    4
  165  139  138  136 1760  115  114  112

 1256    8    8    0    4
  166  140  139  165 1761  116  115 1760

 1257    8    8    0    4
  167  141  140  166 1762  117  116 1761

 1258    8    8    0    4
  168  142  141  167 1763  118  117 1762

 1259    8    8    0    4
  169  143  142  168 1764  119  118 1763

 1260    8    8    0    4
  137  144  143  169  113  120  119 1764

    1    1       1.0       0.0       0.0       0.0
       1.0       1.7     0.866     0.345       0.0       150       0.15
```

```
STOP
```

An explanation of the input parameters and format are given in the DSSIA manual [64].

Vita

Surname: Yao | Given Name: Ming Ming
Place of Birth: Tongbai County, China | *Date of Birth*: Mar. 12, 1979

Educational Institutions Attended

University of Victoria	2000 to 2003
Beijing University of Aeronautics & Astronautics	1995 to 1999

Degree Awarded

B.E.	Beijing University of Aeronautics & Astronautics	1999

Honors

2nd Prize of the Robot Design Competition,	BUAA	1997
1st Prize of the People's Fellowship,	BUAA	1995

Work Experience and Activities in School

Research Assistant	UVic	Sept.2000 to 2003
Lab Instructor	UVic	2001 Fall, 2002 Spring
TA Fellow for organizing Teaching Assistant Training	UVic	July 2002 to June 2003
President of Chinese Scholars and Students Association at UVic		2001/2002

Workshops

Instructional Skills Workshop at the Teaching Innovation Center	UVic	Jan./Feb. 2002
Unigraphics for Aircraft Design, Nanjing University of Aeronautics and Astronautics		Feb. 1999

Conference Presentation

"Dynamic soil-structure-wave interaction of a tall building". Fifth European Conference on Structural Dynamics, Munich, Germany, 2002.

Memberships

Student Member of American Society of Mechanical Engineers	from 2001
Student Member of American Institute of Aeronautics and Astronautics	2001 to 2002
Student Member of International Association for Computational Mechanics	from 2002

Partial Copyright License

Title of Thesis:

Dynamic Wave-Soil-Structure Interaction Analysis

----with Application to Tall buildings

Author: [redacted]

MING MING YAO

August 22, 2003